

## CHAPTER - 5

# *Formulation and Characterization of Ezetimibe Cocrystals*

---

### ABSTRACT

Cocrystallization is one of the approaches to enhance the physicochemical properties of poorly soluble drugs. The aim of this part of study was to evaluate the solubility, release, pharmacokinetic and antihypercholesterolemic characteristics of two new cocrystals (CoCs) of ezetimibe (Eze), prepared using nicotinic acid (NA) and nicotinamide (ND). The ratio of drug:coformer was optimized by solution state studies which included phase solubility and Job's plotting. Eze-NA and Eze-ND CoCs were crystallized using solvents, ethanol and acetone, respectively. CoCs characterization covered flow properties, FTIR, DSC, PXRD, SEM, aqueous solubility, dissolution, pharmacokinetic and antihypercholesterolemic studies. Solution state studies indicated the ratio of Eze:coformer in CoCs. FTIR, DSC and PXRD confirmed the formation of CoCs. SEM pictures showed the distinguished morphology of CoCs as compared to their respective parent components. Cocrystallization significantly ( $p < 0.05$ ) improved the flow property, solubility, dissolution, pharmacokinetic and antihypercholesterolemic properties of Eze. The remarkable enhancement in Eze properties may be attributed to distinguished CoC formation by differential hydrogen bonding of Eze with NA/ND and altered crystal packing style of each CoC.

## **5.1 INTRODUCTION**

Poor solubility of drugs is one of the main challenges in developing oral dosage forms with acceptable bioavailability. 70-90% of the clinically successful drug candidates identified by rationale drug discovery process [Thayer, 2010], 40% of the active pharmaceutical ingredients (APIs) being marketed, and 80% of the drugs being marketed as tablets are classified either as BCS class II or IV (low aqueous solubility) [Goud et al., 2012]. So, solubility improvement plays a crucial role in the development of oral pharmaceutical dosage forms.

Cocrystallization is one of the approaches to enhance solubility and other physicochemical properties of poorly soluble drugs. It is a supramolecular pure crystal engineering technique [Thakuria et al., 2013]. As the pharmaceutical industry prefers crystalline form of API on account of its inherent low energy and thermodynamically stable state, cocrystals (CoCs) are being explored with greater interest at both industrial and academic levels. CoCs not only offer advantages inherent to the crystalline state but, they can be also designed with significantly high aqueous solubility to overcome the solubility limited bioavailability problems of APIs [Mulye et al., 2012; Childs et al., 2013]. A pharmaceutical CoC is a crystalline molecular complex having a distinct solid state, unique structure and physical property profile with an established record of patentability [Trask, 2007; Almarsson et al., 2011].

Cocrystallization modifies the solid-state structural organization and results in powders with finely tuned end-use properties like solubility, dissolution, crystallinity, flowability, melting point, and physical and chemical stability [Gagniere et al., 2009a]. Technically, cocrystallization involves building a periodic crystal lattice out of two or more neutral molecular species that are solids at room temperature, without making or

breaking covalent bonds [Gagniere et al., 2009b]. CoCs form supramolecularly via weak interactions such as hydrogen bonding, van der Waals forces,  $\pi$  stacking, nonionic or other non-covalent bonding. The most likely intermolecular interaction being the hydrogen bonding, selection of the CoC components which usually involve an API and a coformer should ensure the presence of unused hydrogen bond acceptor (e.g., amine or amide groups) and donor (e.g., hydroxyl or carboxylic acid groups) sites in their chemical structures in order to facilitate a mutual bonding [Gao et al., 2012; Lu and Rohani, 2009]. There are a large number of FDA approved GRAS reagents available for exploration as CoC formers [Schultheiss and Newman, 2009]. The present study aims to enhance the solubility and physicochemical properties of ezetimibe (Eze), a model BCS class II drug, by employing two natural CoC formers, nicotinic acid (NA) and nicotinamide (ND).

Eze is a white crystalline powder and its poor aqueous solubility causes high variations in its oral bioavailability [Mulye et al., 2012]. It is the first of its kind hypolipidemic that serves as a cholesterol absorption inhibitor [Shimpi et al., 2014]. To the best of our knowledge, neither NA nor ND has been screened or studied so far, in the development of Eze CoCs. Mulye et al. [2012] was the first to study CoCs of Eze using salicylic acid (SA) and benzoic acid (BA) as CoC forming agents and reported SA to be a better coformer for Eze when compared to BA [Mulye et al., 2012]. Subsequently, Shimpi et al. [2014] prepared CoCs of Eze using L-proline and imidazole [Shimpi et al., 2014] and Sugandha et al. [2014] discovered methyl paraben CoCs of Eze. The L-proline and methyl paraben CoCs were reported with better dissolution behavior compared to pure drug [Shimpi et al., 2014; Sugandha et al., 2014].

Interestingly, Sugandha et al. [2014] reported that there was no interaction between Eze and BA/SA which questions the reports of Mulye et al. [2012]. The prevalence of such conflicting investigations, the fact that none of the above researchers studied the *in-vivo* performance of Eze CoCs and the wide scope of patentability for CoC formulations [Clarke et al., 2009; Frank et al., 2012; Barishansky et al., 2012; Bevill and Schultheiss, 2014] lead to our interest in exploring CoCs of Eze using established and promising cofomers, NA and ND. Literature also suggests that though CoCs are being widely studied, till date, there are only 11 publications that have reported the *in-vivo* performance of CoC systems [Childs et al., 2013].

NA, also known as niacin (vitamin B3), is a lipid lowering agent that acts by inhibiting lipolysis in adipose tissue [Athimoolam and Rajaram, 2005]. NA has been in use in the preparation of CoCs [Kavuru et al., 2010; Sanphui and Rajput, 2014] and we hypothesized that it may offer synergistic hypocholesterolemic effect when formulated with Eze. ND is an amide of niacin. It is not only safe and extensively used in humans but is also considered the most suitable CoC former when solubility and dissolution enhancement is desired, owing to its highly hydrophilic nature [Gagniere et al., 2009a; Gagniere et al., 2009b; Lu and Rohani, 2009; Berry et al., 2008]. The aim of the present work was to prepare NA and ND CoCs of Eze by solution crystallization method [Zhang et al., 2007] and to characterize the CoCs for solid state characters, flow properties, solubility, dissolution and *in-vivo* pharmacokinetic and antihypercholesterolemic activity.

## 5.2 MATERIALS

Eze (purity = 99.3%) was a kind gift from Lupin Ltd. (Pune, India). NA and ND were purchased from Avra Labs Pvt. Ltd. (Hyderabad, India). All other materials of analytical reagent grade were purchased locally and used as received.

## 5.3 METHODS

### 5.3.1 Optimization of composition of ezetimibe – nicotinic acid (Eze-NA) and ezetimibe – nicotinamide (Eze-ND) cocrystals (CoCs)

#### 5.3.1.1 UV-VIS analytical method development for Eze analysis

The first step of the research work was to develop a simple analytical method for the quantification of drug in different drug solutions and formulations prior to proceeding to the preformulation and formulation development experiments. A UV-VIS analytical method was employed for drug content estimation in drug solutions prepared for preformulation studies, in the prepared formulations and also for drug quantification following *in-vitro* tests like solubility and dissolution. Standard calibration curves of Eze were generated in three different media, 0.01 N HCl (pH 2), USP acetate buffer (pH 4.5) and distilled water (measured pH 6.8), to quantify the drug samples.

##### 5.3.1.1.1 Scan for UV-VIS absorption maxima ( $\lambda_{\text{max}}$ ) of Eze

A UV–VIS spectrophotometric analytical method development for Eze analysis was carried out to determine the absorption maxima ( $\lambda_{\text{max}}$ ) of the drug. The UV-VIS absorbance of Eze was examined in three different media, 0.01 N HCl (pH 2), USP acetate buffer (pH 4.5) and distilled water (measured pH 6.8). Two standard solutions of

Eze of increasing concentrations, prepared in each of the media, were scanned on the double beam UV–VIS spectrophotometer (UV–Visible 1800, Shimadzu, Japan) against the respective medium as blank. The procedure for the preparation of standard drug solutions was elaborated in the following section. The  $\lambda_{\text{max}}$  at 232.0 nm was obtained for both the scanned sample standard solutions, in each of the media and hence, this wavelength was selected to prepare the standard calibration curves.

#### **5.3.1.1.2 Preparation of standard calibration curves**

Stock-I standard solution of Eze was prepared by dissolving 25 mg Eze in 25 mL methanol in a volumetric flask. From the stock-I solution of Eze of concentration, 1000  $\mu\text{g/mL}$ , a stock solution-II (100  $\mu\text{g/mL}$  solution) was subsequently prepared using methanol. From stock-II solution, eight different working standard concentrations of Eze were prepared by appropriately diluting the stock-II solution using 0.01 N HCl (pH 2) or USP acetate buffer (pH 4.5) or distilled water (measured pH 6.8) media, to obtain final concentrations, in each of the respective medium. Eze solutions of 2, 4, 6, 8, 10, 15, 20, and 30  $\mu\text{g/mL}$  concentrations were prepared in 10 mL volumetric flasks for constructing a standard calibration curve. Absorbance was measured for each solution against respective blank medium by UV–VIS spectrophotometer at 232 nm. The standard calibration curve was plotted with drug concentration ( $\mu\text{g/mL}$ ) on X-axis and the corresponding UV-VIS mean absorbance values (from six replicate analyses) on Y-axis. Curve fitting was done by linear regression analysis using Microsoft Excel program (Version 2007). The method was validated in terms of linearity, LOD, LOQ, precision (interday and intraday variation) and accuracy.

LOD and LOQ were calculated from the standard calibration curve. From the regression equation of the curve obtained in  $y = mx + c$  form, the slope,  $m$  and the standard

deviation (SD) observed in the y-intercept (c) values, were noted and the following equations, Equations (5.1 and 5.2) were applied:

$$\text{LOD} = 3.3 (\text{SD}/m) \quad \dots\dots\dots \quad \text{Equation 5.1.}$$

and

$$\text{LOQ} = 10 (\text{SD}/m) \quad \dots\dots\dots \quad \text{Equation 5.2.}$$

Precision: Inter-day and intra-day variations were studied to determine the precision of the proposed method. Three different drug concentrations (2, 4 and 10 µg/mL) were prepared in triplicate on three consecutive days and the drug amount was analyzed to determine inter-day precision. For intra-day precision, the same protocol was followed at three different times (0, 6 and 12 h) on the same day. Precision of the developed method was reported as % relative standard deviation (RSD).

Accuracy: For every replicate sample solution prepared to study precision, the accuracy of the developed method was reported as percent recovery (% Recovery) calculated as given below as per Equation (5.3).

$$\% \text{ Recovery} = [(\text{mean found concentration}) / (\text{nominal concentration})] \times 100 \quad \dots\dots\dots \quad \text{Equation 5.3.}$$

### 5.3.1.2 Optimization of the drug:coformer ratio in Eze-NA and Eze-ND CoCs

#### 5.3.1.2.1 Phase solubility studies

Phase solubility was conducted to study the effect of increasing concentrations of CoC formers on the solubility of Eze. The method reported by Higuchi and Connors was followed [Higuchi and Connors, 1965; Nehm et al., 2006; Mulye et al., 2012]. Excess amount of Eze (10 mg) was added to 10 mL distilled water containing 2 – 80 mM NA/ND. The suspensions were continuously shaken on rotary shaker for three days at

room temperature ( $25 \pm 1$  °C) to obtain equilibrium. The suspensions were then filtered, appropriately diluted, and analyzed by UV at 232 nm. The experiments were performed in triplicate and the straight line portions of the phase solubility curves were used to calculate the apparent stability constants (K) of CoCs as per the following equation [same as Equation (2.1)].

$$K = \text{slope}/S_0(1-\text{slope})$$

( $S_0$  is the intrinsic solubility of Eze).

#### **5.3.1.2.2 Job's plot**

Spectrophotometric techniques have been in use in identifying the stoichiometric ratio of components in CoC systems [Shiraki et al., 2008]. Job's plot is a widely used UV-spectrophotometric method that has been in use to identify the stoichiometric ratio of components in a cyclodextrin complex [Misiuk and Zalewska, 2011; Jug et al., 2014]. Correlating the sole involvement of pure intermolecular interactions in the formation of both CoCs and cyclodextrin complexes, this particular method, Job's plot has been applied in this part of study. The stoichiometric ratio of CoC formation between Eze and NA or ND was confirmed by constructing continuous variation Job's plot. The method was experimentally implemented by mixing equimolar solutions of Eze and NA/ND (0.005 mM) in varying molar ratios (1 ml of Eze:9 ml of NA/ND; 2 ml of Eze:8 ml of NA/ND; 3 ml of Eze:7 ml of NA/ND and so on) to a standard volume containing a fixed total concentration of the components. After stirring the mixed solutions of Eze and NA/ND, the absorbance of Eze in each of the solutions was measured at 232 nm by UV. The difference in absorbance in the presence and absence of NA/ND solutions was plotted against R ( $R = [\text{Eze}] / \{[\text{Eze}] + [\text{Coformer}]\}$ ). The maximum difference in the absorbance occurs at the stoichiometric ratio.



### **5.3.2 Preparation and characterization of Eze-NA and Eze-ND CoCs**

#### **5.3.2.1 Preparation of Eze-NA CoCs**

The optimal ratio of Eze:NA in CoC was determined as 1:2 by phase solubility studies as well as Job's plot. 1 mmol Eze and 2 mmol NA were dissolved in 10 mL ethanol and warmed on water bath at 40 °C to obtain clear solution by slow stirring using glass rod. The clear solution was then placed on ice bath at 2 °C for 1 h to induce cocrystallization. Eze-NA CoCs were obtained by air drying the crystallized solutions overnight. The freshly formed CoCs were vacuum oven-dried at 40 °C for 24 h to ensure complete solvent evaporation, then collected and stored in desiccator until further analysis.

#### **5.3.2.2 Preparation of Eze-ND CoCs**

The optimal ratio of Eze:ND in CoC was identified as 1:1 by phase solubility studies and Job's plotting. Eze and ND in equimolar ratio (1 mmol each) were dissolved in 10 mL acetone, warmed on water bath at 40 °C to obtain clear solution by slow stirring using glass rod. The clear solution was then placed on ice bath at 2 °C for 1 h to induce cocrystallization. Overnight air drying produced fresh Eze-ND CoCs that were vacuum oven-dried at 40 °C for 12 h to ensure complete solvent evaporation. The CoCs were then collected and stored in desiccator for further analysis.

### **5.3.2.3 Stoichiometric assay**

The CoC stoichiometry was confirmed by assaying the contents of drug and coformer in the studied CoC solid forms by employing UV-Vis spectrophotometric analysis [Gao et al., 2011].

#### **5.3.2.3.1 UV-VIS analytical method development and validation for NA analysis**

A simple UV analytical method was developed for the quantification of NA content in Eze-NA CoC formulation. Standard calibration curve of NA was generated in distilled water to quantify the samples.

##### **5.3.2.3.1.1 Scan for UV-VIS absorption maxima ( $\lambda_{\max}$ ) of NA**

A UV–VIS spectrophotometric analytical method development for NA analysis was carried out. The UV-VIS absorbance of NA was examined to determine the absorption maxima ( $\lambda_{\max}$ ) of NA in distilled water. Analysis by UV–VIS spectrophotometry showed a characteristic peak corresponding to NA at 263.0 nm. Three standard solutions of NA of increasing concentrations, prepared in distilled water, were scanned on the double beam spectrophotometer against the respective medium as blank. The  $\lambda_{\max}$  at 263.0 nm was obtained for the scanned sample standard solutions and hence, this wavelength was selected to prepare the standard calibration curve. Standard NA solutions in distilled water were analyzed in the concentration range of 6 – 30  $\mu\text{g/mL}$ .

##### **5.3.2.3.1.2 Preparation of standard calibration curve**

Stock-I standard solution of NA was prepared by dissolving 25 mg NA in 25 mL distilled water in a volumetric flask. From the stock-I solution of NA of concentration, 1000  $\mu\text{g/mL}$ , a stock solution-II (100  $\mu\text{g/mL}$  solution) was subsequently prepared. From stock-II solution, six different working standard concentrations of NA were prepared by

appropriately diluting the stock-II solution using distilled water, to obtain final concentrations. NA solutions of 6, 8, 10, 15, 20, and 30  $\mu\text{g/mL}$  concentrations were prepared in 10 mL volumetric flasks for constructing a standard calibration curve. Absorbance was measured for each solution against distilled water blank by UV–VIS spectrophotometry at 263.0 nm. The standard calibration curve was plotted with NA concentration ( $\mu\text{g/mL}$ ) on X-axis and the corresponding UV-VIS mean absorbance values (from six replicate analyses) on Y-axis. Curve fitting was done by linear regression analysis using Microsoft Excel program (Version 2007). The method was validated in terms of linearity, LOD, LOQ, precision (inter day and intraday variation) and accuracy.

Precision: Inter-day and intra-day variations were studied to determine the precision of the proposed method. Three different drug concentrations (6, 10 and 20  $\mu\text{g/mL}$ ) were prepared in triplicate on three consecutive days and the drug amount was analyzed to determine inter-day precision. For intra-day precision, the same protocol was followed at three different times (0, 6 and 12 h) on the same day. Precision of the developed method was reported as % RSD.

Accuracy: For every replicate sample solution prepared to study precision, the accuracy of the developed method was reported as % Recovery.

#### **5.3.2.3.2 UV-VIS analytical method development and validation for ND analysis**

A simple UV analytical method was developed for the quantification of ND content in Eze-ND CoC formulation. Standard calibration curve of ND was generated in distilled water to quantify the samples.

**5.3.2.3.2.1 Scan for UV-VIS absorption maxima ( $\lambda_{\max}$ ) of ND**

A UV–VIS spectrophotometric analytical method development for ND analysis was carried out. The UV-VIS absorbance of ND was examined to determine the absorption maxima ( $\lambda_{\max}$ ) of ND in distilled water. Analysis by UV–VIS spectrophotometry showed a characteristic peak corresponding to ND at 262.0 nm. Three standard solutions of ND of increasing concentrations, prepared in distilled water, were scanned on the double beam spectrophotometer against the respective medium as blank. The  $\lambda_{\max}$  at 262.0 nm was obtained for the scanned sample standard solutions and hence, this wavelength was selected to prepare the standard curve. Standard ND solutions in distilled water were analyzed in the concentration range of 4 – 20  $\mu\text{g/mL}$ .

**5.3.2.3.2.2 Preparation of standard calibration curve:**

Stock-I standard solution of ND was prepared by dissolving 25 mg ND in 25 mL distilled water in a volumetric flask. From the stock-I solution of ND of concentration, 1000  $\mu\text{g/mL}$ , a stock solution-II (100  $\mu\text{g/mL}$  solution) was subsequently prepared. From stock-II solution, six different working standard concentrations of ND were prepared by appropriately diluting the stock-II solution using distilled water, to obtain final concentrations. ND solutions of 4, 6, 8, 10, 15 and 20  $\mu\text{g/mL}$  concentrations were prepared in 10 mL volumetric flasks for constructing a standard calibration curve. Absorbance was measured for each solution against distilled water blank by UV–VIS spectrophotometry at 262.0 nm. The standard calibration curve was plotted with ND concentration ( $\mu\text{g/mL}$ ) on X-axis and the corresponding UV-VIS mean absorbance values (from six replicate analyses) on Y-axis. Curve fitting was done by linear regression analysis using Microsoft Excel program (Version 2007). The method was

validated in terms of linearity, LOD, LOQ, precision (interday and intraday variation) and accuracy.

**Precision:** Inter-day and intra-day variations were studied to determine the precision of the proposed method. Three different drug concentrations (4, 10 and 20 µg/mL) were prepared in triplicate on three consecutive days and the drug amount was analyzed to determine inter-day precision. For intra-day precision, the same protocol was followed at three different times (0, 6 and 12 h) on the same day. Precision of the developed method was reported as % RSD.

**Accuracy:** For every replicate sample solution prepared to study precision, the accuracy of the developed method was reported as % Recovery.

#### **5.3.2.3.3 Stoichiometric assay procedure**

The Eze-NA CoC stoichiometry was determined after preparation of the solid form CoC, for confirmation purpose. Three batches of 10 mg CoC were dissolved in 5 mL methanol, sonicated for 1 min and filtered. After appropriate dilutions, the solutions were assayed for Eze content by UV at 232 nm and the average was noted. Similarly, another fraction of 10 mg CoC was dissolved in 5 mL water, sonicated for 1 min and filtered. After appropriate dilutions, the solutions were assayed for NA content by UV at 263 nm. The readings were taken in triplicate and the average was noted.

The stoichiometry of Eze-ND CoC was determined after preparation of the solid form CoC, for confirmation purpose. Three batches of 10 mg CoC were dissolved in 5 mL methanol, sonicated for 1 min and filtered. After appropriate dilutions, the solutions were assayed for Eze content by UV at 232 nm and the average was noted. Similarly, another fraction of 10 mg CoC was dissolved in 5 mL water, sonicated for 1 min and

filtered. After appropriate dilutions, the solutions were assayed for ND content by UV at 262 nm. The readings were taken in triplicate and the average was noted.

#### **5.3.2.4 Solid state characterization**

##### **5.3.2.4.1 Fourier transform infra-red (FTIR) spectroscopy**

FTIR spectra were recorded using FTIR spectrophotometer (FTIR-8400S, Shimadzu Co., Kyoto, Japan). Samples were prepared by cogrinding with anhydrous KBr powder and compressing the mixture into pellets. The FTIR spectra were measured over the range of 4000-400  $\text{cm}^{-1}$ .

##### **5.3.2.4.2 Differential scanning calorimetry (DSC)**

DSC analysis was performed using DSC-822<sup>e</sup> (TGA/DSC-1, Mettler Toledo, AG, Analytical, Switzerland) with STAR<sup>e</sup> evaluation software. 4-7 mg samples were accurately weighed in aluminium pans and heated between 10 °C and 300 °C.

##### **5.3.2.4.3 Powder X-Ray diffraction (PXRD) analysis**

X-Ray diffraction (XRD) patterns were traced by employing X-ray diffractometer (PW3050/60 X'pert PRO, PANalytical, Netherlands) with Cu anode at 40 kV and 30 mA. The data was collected at 25 °C in the range  $0^{\circ} < 2\theta < 80^{\circ}$ .

##### **5.3.2.4.4 Scanning electron microscopy (SEM)**

The surface morphological properties were investigated by SEM (FEI, QUANTA-200, Netherlands) and the photographs were taken at an accelerating voltage of 20 kV.

##### **5.3.2.4.5 Thermogravimetric Analysis (TGA)**

TGA was performed using TGA/DSC-1, STAR<sup>e</sup> system (Mettler Toledo, Switzerland) to understand the weight loss behavior with the increase in temperature. About 2 mg samples were accurately weighed and placed on open aluminum pan suspended in a

heating furnace. The sample weight loss was monitored at a heating rate of 10 °C/min and in the range of 10 °C to 350 °C under continuous nitrogen purging at 10 mL/min.

#### **5.3.2.5 Flow properties**

The flow properties of Eze and CoCs, in terms of, angle of repose (AR), Carr's index (CI) and Hausner's ratio (HR), were determined and statistically validated (n=3). Fixed funnel method was used to study AR. CI and HR were calculated from bulk and tapped density values.

#### **5.3.2.6 Drug content**

Known amounts of drug and CoCs equivalent to 10 mg of drug were dissolved in 5 mL methanol, sonicated for 1 min and filtered. After appropriate dilutions, the solutions were assayed for Eze content by UV at 232 nm. The readings were taken in triplicate and the average was noted.

#### **5.3.2.7 Saturation aqueous solubility studies**

Excess amounts of drug and CoCs were added to 10 mL distilled water. The suspensions were shaken continuously on rotary shaker for 24 h at room temperature, filtered and the drug amount was measured by UV at 232 nm.

#### **5.3.2.8 Dissolution**

The dissolution media suggested for Eze (marketed tablet formulation) by the FDA "Dissolution Methods" guidelines was USP acetate buffer of pH 4.5 containing 0.45% w/v sodium lauryl sulfate (SLS). The same USFDA method of dissolution was adapted

with modifications

[[http://www.accessdata.fda.gov/scripts/cder/dissolution/dsp\\_SearchResults\\_Dissolution.s.cfm?PrintAll=1](http://www.accessdata.fda.gov/scripts/cder/dissolution/dsp_SearchResults_Dissolution.s.cfm?PrintAll=1)]. The dissolution studies were carried out by filling 10 mg of pure drug, physical mixtures (PMs) and each of the formulations equivalent to 10 mg of Eze into hard gelatin capsules. The dissolution medium used was 500 mL USP acetate buffer of pH 4.5 containing 0.45% w/v SLS and dissolution was conducted using USP apparatus I (Electrolab, India) at  $37\pm 0.5$  °C and 100 rpm rotation rate. 5 mL samples were withdrawn at appropriate time intervals and the medium volume was made up to 500 mL by replacing the withdrawn samples with fresh prewarmed ( $37\pm 0.5$  °C) medium. The collected samples were filtered, appropriately diluted and Eze content was quantified by UV at 232 nm. The cumulative percent drug dissolved at each time point was calculated for pure drug, PMs and each of the formulations and the data obtained by six replicate determinations was averaged and recorded. Dissolution was studied for 120 min and the dissolution efficiency (DE) representing the area under the dissolution curve up to 120 min was calculated for each of the systems. Additionally,  $t_{80\%}$  and  $t_{90\%}$  values were noted for the CoCs.

### 5.3.2.9 Stability

The well optimized CoCs, Eze-NA and Eze-ND were subjected to stability studies at  $30\pm 2$  °C/ $70\pm 5\%$  RH for 6 months, as per the ICH (International Conference on Harmonization) guideline, Q1A(R2), ASEAN (The Association of Southeast Asian Nations) and WHO proposals for the finished pharmaceutical products (FPPs) of climatic zone IV A (hot and humid). The stability testing conditions observed were in accordance with the conditions ( $30$  °C/ $70\%$  RH) recommended by the Regional Office



for South-East Asia (SEARO) for the WHO member state, India, in particular [WHO technical report series no. 953].

Six batches of freshly prepared and dried CoCs, each of Eze-NA and Eze-ND, were stored in air-tight glass vials, sealed and placed in stability chamber (Narang Industries, New Delhi, India) at  $30\pm 2$  °C/ $70\pm 5\%$  RH. The freshly prepared batches were tested mainly for drug content, solubility and dissolution tests and the results were noted. After 6 months, the samples were withdrawn and evaluated for drug content, aqueous solubility and dissolution properties and the results obtained were examined by comparing the values noted before and after 6 months.

### 5.3.2.10 *In-vivo* preclinical pharmacokinetic study

#### 5.3.2.10.1 Animals

The study protocol was approved and guided by the Central Animal Ethical Committee, Institute of Medical Sciences, Banaras Hindu University, Varanasi, India. Male Albino Wister rats (200 – 250 g) were used and the animals were divided into three groups of six animals each. The standard - group I, test - group II, and test – group III, received pure drug suspension, Eze-ND, and Eze-NA, respectively. The animals were housed in polypropylene cages and kept at standard laboratory conditions ( $25\pm 2$  °C and  $55\pm 5\%$  RH). Six animals per cage were accommodated with free access to standard laboratory diet (Lipton feed, Mumbai, India) and water *ad libitum*.

#### 5.3.2.10.2 Dosing and sampling

All the animals used were fasted overnight for the study and dosed orally using 18-gauge oral feeding needle. A single dose pharmacokinetic study was conducted and all the treatment group animals received 2 mL of 50 mg/kg body weight equivalent dose of

Eze, via oral administration. The animal groups, I, II, and III, received pure drug, Eze-ND, and Eze-NA, respectively, dispersed in 0.25% w/v sodium carboxymethylcellulose (NaCMC). After anaesthetizing the rats with diethyl ether, 500  $\mu$ L blood samples were collected by retro-orbital puncture at 0 (pre-dose), 0.5, 1, 1.5, 2, 2.5, 4, 12, and 24 h, into heparinized microcentrifuge tubes. After blood sampling at each time point, the blood loss was compensated by immediately injecting same volume of normal saline. Plasma was immediately separated by centrifugation at 5000 rpm for 20 min, spiked with internal standard (IS), nitrendipine, and stored at -20 °C until bioanalysis.

### 5.3.2.10.3 Drug extraction

A previously reported and established extraction procedure was observed as per the following principle [Bali et al., 2010 and 2011; Suchy et al., 2013]. Upon oral administration, the absorbed Eze is extensively conjugated to Ezetimibe-Phenoxy glucuronide (EzeG), a pharmacologically active metabolite. Both Eze and EzeG, respectively, constitute approximately 10-20% and 80-90% of the total drug detected in plasma. Owing to the very low amounts of detectable free drug in plasma, the drug quantification was carried out by incorporating a glucuronide hydrolysis step. Addition of  $\beta$ -glucuronidase (minimum 100,000 units/mL) to the plasma samples aided in the conversion of EzeG to Eze and the total Eze (free plasma Eze + plasma EzeG) in plasma was estimated and reported. The plasma Eze extraction procedure observed was as described below.

The stored plasma samples containing drug and IS (Nitrendipine was used as IS as per previously reported method; the concentration of standard working analytical IS solution used for spiking was precalculated so as to maintain a constant final plasma concentration of 100 ng/mL), were thawed at ambient temperature for proceeding to

drug separation and quantification. 100  $\mu\text{L}$  aliquots of plasma were transferred to 5 mL eppendorf tubes to facilitate the extraction procedure. In order to extract total Eze (free and conjugated), 250  $\mu\text{L}$  0.5 M sodium acetate buffer (pH 5.0 with glacial acetic acid) and 25  $\mu\text{L}$   $\beta$ -glucuronidase (minimum 100,000 units/mL) were added, vortex-mixed for 30 s and incubated for 4 h at 50 – 55  $^{\circ}\text{C}$  to induce EzeG hydrolysis. Post incubation, 250  $\mu\text{L}$  0.1 M sodium borate buffer (pH 9.8 with triethylamine) was added and vortexed for 30 s to terminate the hydrolysis reaction. The solution was left until it cooled to room temperature. Total Eze was then extracted by adding 1.5 mL methyl tertiary butyl ether and vortex mixing for 90 s. The tubes were centrifuged at 3000 rpm for 15 min and 10  $^{\circ}\text{C}$ . Organic layer was separated, filtered through 0.45  $\mu\text{m}$  filter and evaporated while immersed in water bath at 40  $^{\circ}\text{C}$  and left until completely dry. The dry residue was dissolved in 1 mL methanol and again evaporated to dryness. Residue was finally reconstituted in 100  $\mu\text{L}$  mobile phase and 20  $\mu\text{L}$  of reconstituted samples were filtered through 0.2  $\mu\text{m}$  syringe filter, injected into the column and the drug amount was quantified. Plasma drug quantification of Eze was carried out using a HPLC-UV method that has been previously reported in literature and the estimated drug values were applied to study the pharmacokinetics. For the purpose of plasma Eze quantification, a HPLC-UV standard calibration curve was constructed by spiking the plasma samples with known concentrations of Eze.

#### **5.3.2.10.4 Plasma drug analysis**

##### **5.3.2.10.4.1 HPLC-UV method development for plasma drug analysis**

In order to study the preclinical rat pharmacokinetic experiments, a suitable analytical method was developed and validated for the quantification of drug in rat plasma. A HPLC-UV bioanalytical method was employed for drug content estimation in rat

plasma following single dose pharmacokinetic studies. Two standard calibration curves of Eze were generated using analytical and bioanalytical drug samples to aid in drug quantification in plasma samples. Eze solutions were analyzed in the concentration range of 100 – 8000 ng/mL. Drug detection by HPLC-UV (Shimadzu Corporation, koyoto, Japan) was accomplished using characteristic UV-VIS absorbance wavelength corresponding to Eze at 232 nm for analytical and bioanalytical drug solutions.

A validated HPLC-UV bioanalytical method for pharmacokinetic studies of free Eze in human volunteers has been reported in literature and the same was adopted with modifications in the present study [Suchy et al., 2013]. The principle behind the modifications observed in the bioanalytical method employed in this study was as follows. The method already reported in literature was applied to study the multiple oral dose pharmacokinetics of Eze and to estimate the amount of free Eze in human volunteers. In contrast, the present research work aimed to study the single oral dose pharmacokinetics of Eze in male Albino Wister rats. Moreover, since the Eze absorbed following oral administration gets extensively conjugated to EzeG, a pharmacologically active metabolite, the amounts of free Eze detectable in plasma would be very low. Both Eze and EzeG, respectively, constitute approximately 10-20% and 80-90% of the total drug detected in plasma. As the amounts of detectable free drug in plasma would be very low, the drug quantification was carried out by estimating total Eze (free plasma Eze + plasma EzeG) by following glucuronide hydrolysis method. So, the total plasma Eze analysis by HPLC-UV encountered one major problem that is the conversion of EzeG to Eze by enzymatic hydrolysis by simultaneously ensuring minimal interference from either the endogenous components of enzyme or plasma components. To overcome this problem, the amount of enzyme to be added was selected based on the

previously reported methods [Gaikwad and Bhoir, 2013; Gaikwad et al., 2013]. Thus selected enzyme concentration ensured optimal enzymatic reaction and optimal recovery of Eze for detection by HPLC-UV. The final concentrations of total Eze (free plasma Eze + plasma EzeG) were subjected to pharmacokinetic and statistical analysis.

#### **5.3.2.10.4.2 Chromatographic conditions**

The HPLC system (Shimadzu Corporation, Kyoto, Japan) employed was equipped with a UV-Visible detector (SPD-20A), two delivery pumps (LC-20AD), a degasser (DGU-20A3) and a Rheodyne manual injector (SIL-20A) provided with 20  $\mu$ L sample loop for sample loading. A Phenosphere C18 reverse-phase column, 250 $\times$ 4.6 mm and 5  $\mu$ m packing (Phenomenex, Sydney, Australia), attached to a C18 guard column was used for drug separation. Mobile phase composition was 60:40 v/v acetonitrile and 0.1 M ammonium acetate aqueous solution. Isocratic elution of samples (20  $\mu$ L injection volumes) was performed at 1 mL/min flow rate and the eluent absorption was monitored at 232 nm constant UV wavelength. Mobile phase was deaerated using bath sonicator and then filtered through 0.2  $\mu$ m syringe filter before injection by Hamilton syringe into HPLC column.

#### **5.3.2.10.4.3 Analytical HPLC-UV method development – preparation of standard calibration curve for pure drug solutions**

Drug solutions were analyzed in the concentration range of 100 – 8000 ng/mL. Stock solutions, I (1000  $\mu$ g/mL), II (100  $\mu$ g/mL), and III (10  $\mu$ g/mL) of Eze were prepared using HPLC grade methanol. From stock solution III, eight different working concentrations of Eze, 100, 200, 400, 800, 1000, 2000, 4000, and 8000 ng/mL, were prepared in 1 mL microcentrifuge (Eppendorf) tubes after appropriate dilutions using mobile phase as media for constructing the standard calibration curve. 20  $\mu$ L samples

were filtered through 0.2 µm syringe filter, injected into the HPLC column and the drug amount was quantified to obtain the standard calibration curve. The standard calibration curve was plotted with drug concentration (ng/mL) on X-axis and the corresponding HPLV-UV mean drug peak area values (from six replicate analyses) on Y-axis. Curve fitting was done by linear regression analysis using Microsoft Excel program (Version 2007).

The method was validated in terms of linearity, LOD, LOQ, precision (inter day and intraday variation) and accuracy. The precision and accuracy in case of HPLC method validation were studied for 200, 400 and 1000 ng/mL concentrations of working solutions. Pure drug solutions of concentrations, 200, 400 and 1000 ng/mL of Eze, were analyzed for inter-day and intra-day precision of the developed method. Three replicates at each concentration were prepared as described above, on days, 1, 2 and 3, for evaluating inter-day precision. For intra-day precision, samples were prepared on the same day at different times, 0, 6 and 12 h. For every replicate sample solution prepared to study precision, the accuracy of the developed method was reported as % Recovery.

#### ***5.3.2.10.4.3.1 Determination of extraction efficiency of the developed analytical***

##### ***HPLC-UV method - preparation of plasma spiked drug solutions***

Plasma drug solutions of final concentrations, 200, 400 and 1000 ng/mL of Eze were prepared to study the extraction efficiency of the developed analytical HPLC-UV method. Back calculated known concentrations of working standard drug solutions were prepared from stock solutions as described in the previous section. 100 µL drug free plasma samples (control or blank plasma) were spiked with appropriate volumes of respective working standard drug solutions to obtain the final plasma drug concentrations of 200, 400 and 1000 ng/mL.

**5.3.2.10.4.3.2 Drug extraction procedure**

An established extraction procedure was followed to extract Eze from spiked plasma samples [Bali et al., 2010 and 2011] as described under the section 5.3.2.10.3. The procedure followed was the same as observed for extraction of drug from the pharmacokinetic plasma drug samples in order to ensure the suitability of the developed HPLC-UV method for plasma drug analysis following pharmacokinetic studies.

**5.3.2.10.4.3.3 Extraction efficiency (EE)**

The drug EE of the developed HPLC-UV analytical method was determined for plasma drug concentrations of 200, 400 and 1000 ng/mL. Three replicates of each sample extracted and analyzed as described above were compared with unextracted drug samples to determine the possible bias in HPLC-UV quantification of Eze in the analytical and bioanalytical drug samples. The EE at each concentration was calculated as given below as per Equation (5.4):

$$EE = \left[ \frac{\text{Peak area after extraction from drug solution spiked plasma}}{\text{Peak area after direct injection of drug solution}} \right] \times 100 \quad \dots\dots\dots \text{Equation 5.4.}$$

**5.3.2.10.4.4 Bioanalytical HPLC-UV method development – preparation of standard calibration curve with plasma spiked drug solutions**

Standard plasma drug solutions were also analyzed in the final working plasma drug concentration range of 100 – 8000 ng/mL of Eze. Nitrendipine solution of final working plasma drug concentration, 100 ng/mL, was employed as IS. Eze and IS stock solutions were prepared using HPLC grade methanol and the required concentrations of working standard solutions were back calculated and prepared by appropriate dilution of stock-III (10 µg/mL) solution with the mobile phase and the same were used for preparing standard spiked plasma drug solutions. The bulk drug free plasma collected was stored

at -20°C until bioanalysis and thawed just before use. The standard plasma drug solutions were prepared by spiking 100 µL plasma samples with drug and IS.

Eight separate 100 µL drug free plasma samples (control or blank plasma) were spiked with appropriate volumes of known respective working drug solutions to obtain the final plasma drug concentrations in the range of 100 – 8000 ng/mL of Eze, each containing a constant 100 ng/mL of IS. Eight different working plasma concentrations of Eze, 100, 200, 400, 800, 1000, 2000, 4000, and 8000 ng/mL, were prepared by spiking followed by careful extraction and final reconstitution using mobile phase as media for constructing the standard plasma drug calibration curve.

The extraction procedure was the same as described in the above section except here, the 100 µL aliquots of plasma were spiked with working standards of drug as well as IS solutions of known concentrations (IS of known concentration to obtain a final and constant 100 ng/mL plasma concentration) before transfer into 5 mL eppendorf tubes. 20 µL of extracted and reconstituted (using mobile phase) samples were filtered through 0.2 µm syringe filter, injected into the HPLC column and the drug amount was quantified to obtain the standard plasma drug calibration curve. An eight-point standard plasma drug calibration curve was obtained in the final plasma drug concentration range of 100 – 8000 ng/mL. The standard calibration curve was plotted with drug concentration (ng/mL) on X-axis and the corresponding HPLV-UV mean peak area ratio values of Eze:IS (from six replicate analyses) on Y-axis. Curve fitting was done by linear regression analysis using Microsoft Excel program (Version 2007). The method was validated in terms of linearity, LOD, LOQ, precision (inter day and intraday variation) and accuracy.



Plasma drug solutions of final concentrations, 200, 400 and 1000 ng/mL of Eze were analyzed for inter-day and intra-day precision of the developed method. Three replicates at each concentration were prepared as described above, on days, 1, 2 and 3, for evaluating inter-day precision. For intra-day precision, samples were prepared on the same day at different times, 0, 6 and 12 h. For every replicate sample solution prepared to study precision, the accuracy of the developed method was reported as % Recovery.

### 5.3.2.10.5 Pharmacokinetic parameters

Pharmacokinetic parameters such as peak plasma concentration ( $C_{max}$ ), time to reach the peak plasma concentration ( $T_{max}$ ), area under the plasma concentration-time curve till time,  $t$ , ( $AUC_{0-t}$ ) and infinite time, ( $AUC_{0-\infty}$ ), area under the first moment curve till time,  $t$ , ( $AUMC_{0-t}$ ), and mean residence time (MRT) were computed for each group by non-compartmental pharmacokinetic model using Kinetica 5.0 pharmacokinetic software (Trial version, PK-PD analysis, Thermofischer) and Graphpad Prism software (version 5.03, GraphPad Software, USA).

### 5.3.2.11 Antihypercholesterolemic activity

The Central Animal Ethical Committee, Institute of Medical Sciences, Banaras Hindu University, Varanasi, India, approved and guided the study protocol. Male Albino Wister rats of 200 – 250 g were used and six animals per cage were accommodated in polypropylene cages, maintained at  $25 \pm 2$  °C and  $55 \pm 5\%$  RH, with free access to standard laboratory diet (Lipton feed, Mumbai, India) and water *ad libitum*. The animals were divided into four groups each of six animals. The control - group I, standard - group II, test – group III, test – group IV, test – group V and test – group VI received cholesterol, pure drug suspension plus cholesterol, pure NA plus cholesterol,

Eze-NA PM plus cholesterol, Eze-NA plus cholesterol, and Eze-ND plus cholesterol, respectively.

The study was carried out for total period of 8 weeks wherein the first four weeks, all the animals were fed 200 mg cholesterol in 2 mL coconut oil as high fat diet for inducing hypercholesterolemia [Dixit and Nagarsenker, 2008; Bandyopadhyay et al., 2012]. At the end of fourth week, the plasma cholesterol levels were measured for all the groups and the values were considered as baseline values for the following four week study, the actual antihypercholesterolemic activity study. The first four weeks is a stage 1, hypercholesterolemic induction study and the next four weeks is the stage 2, antihypercholesterolemic activity study.

Antihypercholesterolemic activity was carried out for 28 days and the animals were fed orally using 18-gauge oral feeding needle. The daily dose was calculated by considering the surface area ratio of rat to human being. All the groups were induced with hypercholesterolemia by feeding high fat diet (200 mg cholesterol in 2 mL coconut oil) [Dixit and Nagarsenker, 2008; Bandyopadhyay et al., 2012]. Two hours following the administration of high fat diet, the treatment groups, II, III, IV, V and VI were respectively fed with pure drug, pure NA, Eze-NA PM, Eze-NA and Eze-ND, dispersed in 0.25% w/v NaCMC. Volume of vehicle (200  $\mu$ L) and dose levels of 1 mg Eze or equivalent formulation/kg body weight/day were kept constant in each case. For pure NA group, the dose was equivalent to the amount of NA in 1 mg Eze equivalent weight of Eze-NA CoC. Blood samples were collected into heparin treated microcentrifuge tubes by retro-orbital puncture on day 7, 14, 21 and 28, after anaesthetizing the rats with diethyl ether. Plasma was separated by centrifuging at 5000 rpm for 20 min and stored

at 2 °C until further use. Percent reduction in the levels of total plasma cholesterol was analysed using *in-vitro* Cogent diagnostic kit (Span Diagnostics Ltd., Surat, India).

### **5.3.2.12 Statistical analysis**

The results were shown as Mean $\pm$ SD. The data pertaining to flow properties, solubility, dissolution and pharmacokinetic studies were analyzed by one-way analysis of variance (ANOVA) followed by post hoc Tukey multiple comparison test ( $p < 0.05$ ). The antihypercholesterolemic study results were analyzed by two-way ANOVA followed by post hoc Bonferroni multiple comparison test ( $p < 0.05$ ).

## **5.4 RESULTS AND DISCUSSION**

### **5.4.1 Optimization of composition of Eze-NA and Eze-ND CoCs**

#### **5.4.1.1 UV-VIS Eze analysis – method development and validation**

A simple UV spectrophotometric method was developed for drug quantification for use in *in-vitro* drug content estimation in preformulation drug samples, in prepared formulations, and for studying solubility and dissolution test results. Working standard concentrations of Eze were prepared using three different media, 0.01 N HCl (pH 2), USP acetate buffer (pH 4.5) and distilled water (measured pH 6.8). The solutions were scanned for  $\lambda_{\max}$  of the drug and it was found that Eze exhibited maximum absorption at two wavelengths, 232.0 nm and 247.0 nm. Literature suggested 232.0 nm as the most acceptable UV-VIS  $\lambda_{\max}$  of Eze.

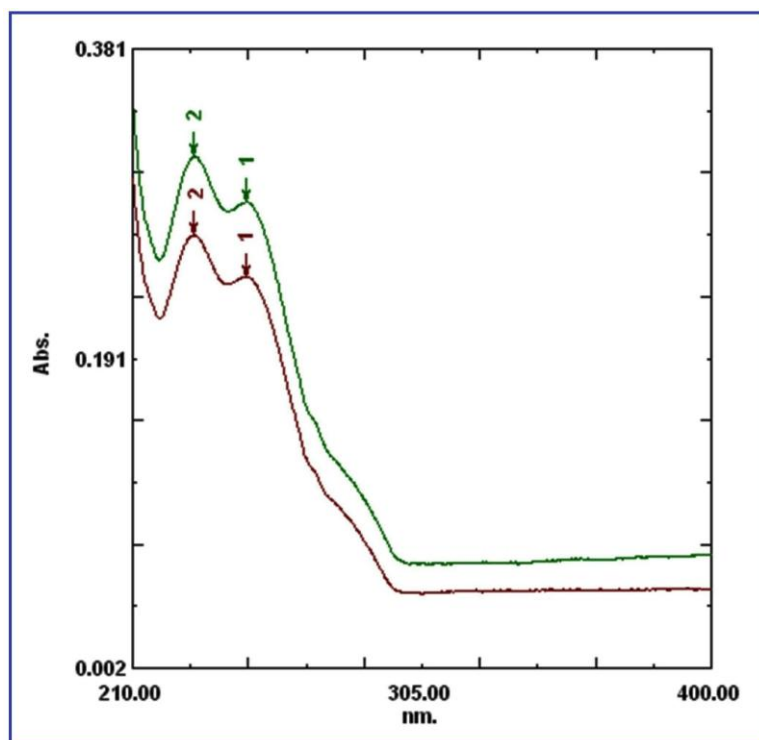


Figure 5.1. UV-VIS spectral scan of pure Eze in 0.01 N HCl (pH 2).

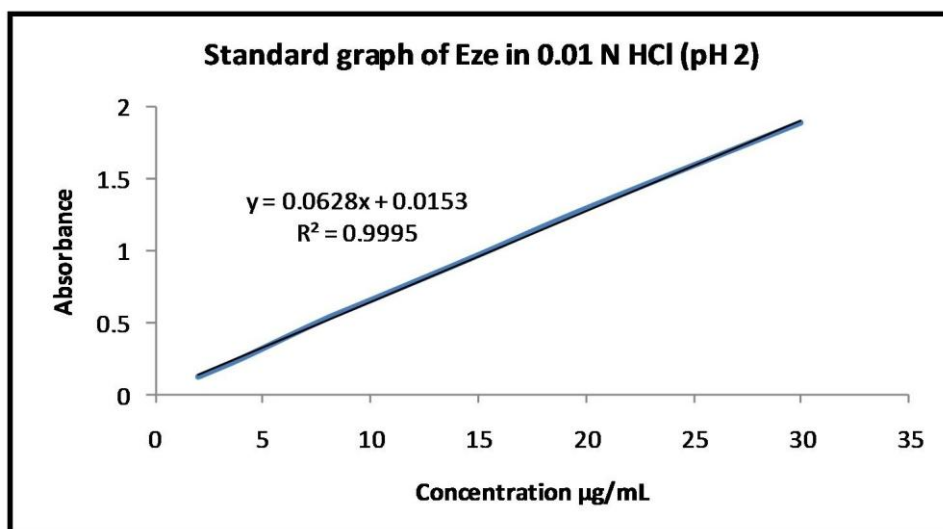


Figure 5.2. UV-VIS standard calibration curve of pure Eze in 0.01 N HCl (pH 2).

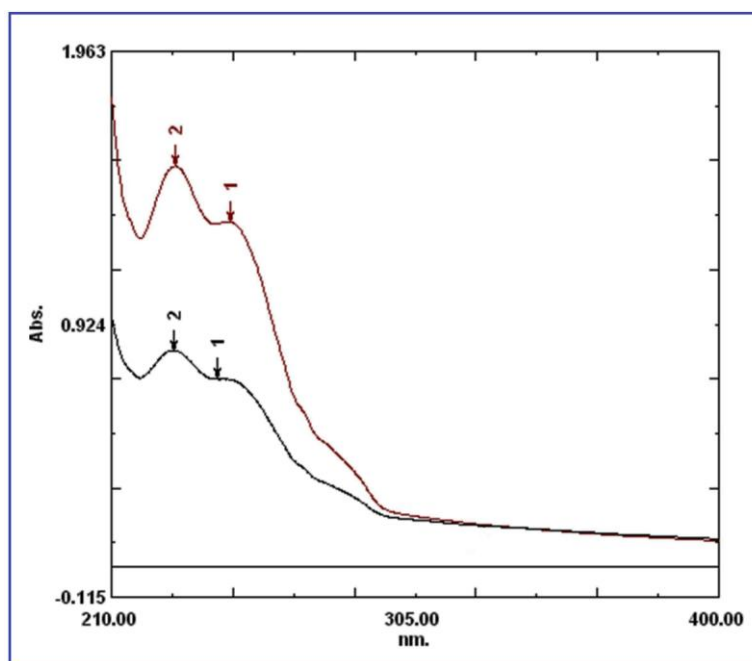


Figure 5.3. UV-VIS spectral scan of pure Eze in USP acetate buffer (pH 4.5).

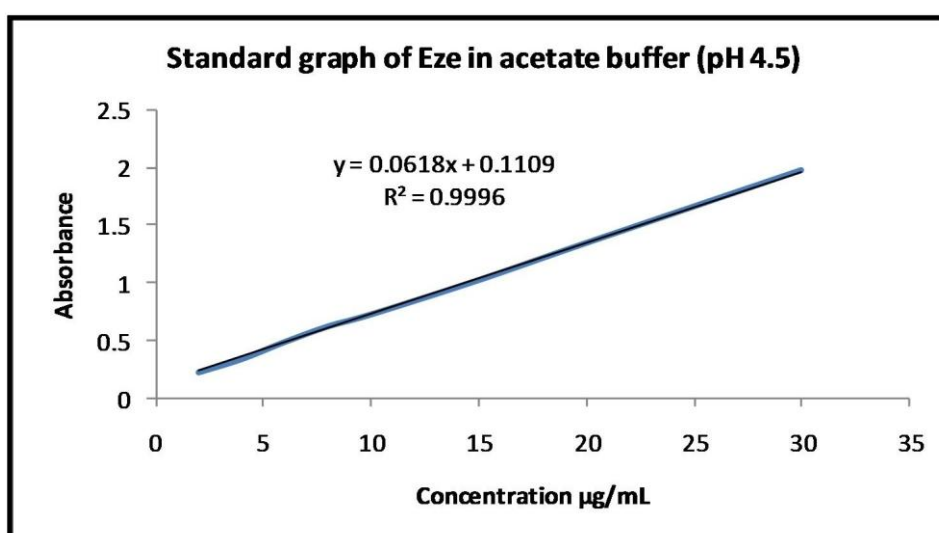


Figure 5.4. UV-VIS standard calibration curve of pure Eze in USP acetate buffer (pH 4.5).

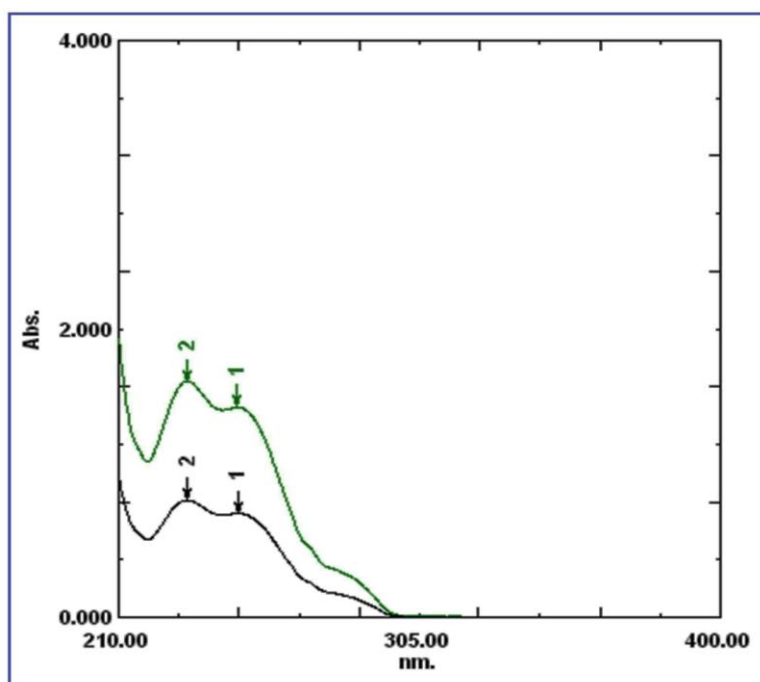


Figure 5.5. UV-VIS spectral scan of pure Eze in distilled water (measured pH 6.8).

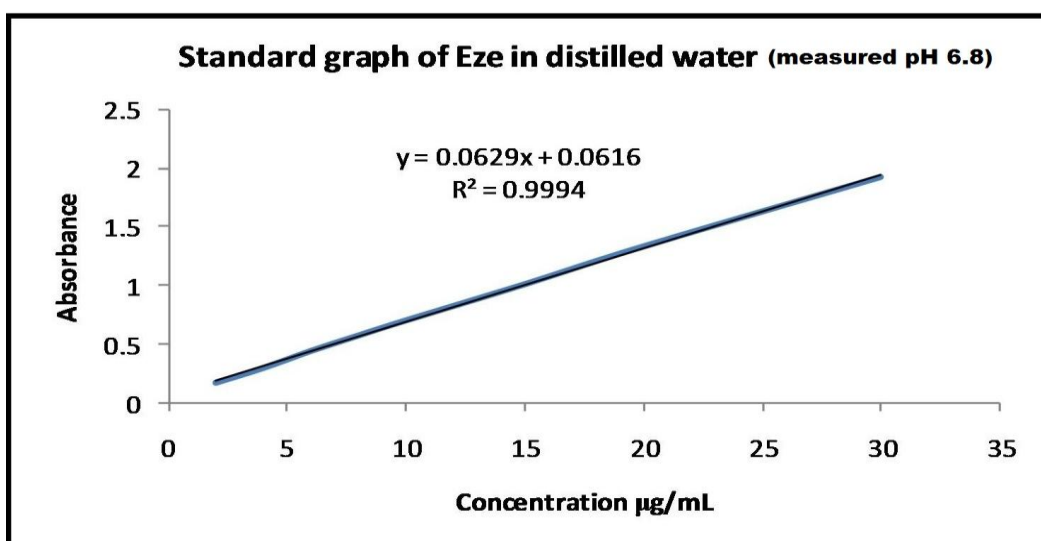


Figure 5.6. UV-VIS standard calibration curve of pure Eze in distilled water (measured pH 6.8).

Standard UV–VIS calibration curves of Eze were generated in all the three media, 0.01 N HCl (pH 2), USP acetate buffer (pH 4.5) and distilled water (measured pH 6.8), to quantify the samples in the concentration range of 2 – 30 µg/mL at 232 nm. The UV-VIS spectral scans of standard Eze solutions prepared using different media were presented in Figures, 5.1, 5.3 and 5.5 and the respective UV-VIS standard calibration curves were shown in Figures, 5.2, 5.4 and 5.6.

The regression equation for pure Eze samples in all the three media, 0.01 N HCl (pH 2), USP acetate buffer (pH 4.5) and distilled water (measured pH 6.8), was obtained in the form,  $y = mx + c$ , where  $y$  represents the Eze absorbance,  $x$  represents the concentration of Eze,  $m$  is the slope of the plot, and  $c$  is the intercept, in each of the respective medium. The standard calibration curve was found to be linear throughout the concentration range studied in each of the three media.

The regression equation for pure Eze samples in 0.01 N HCl (pH 2) from the corresponding eight-point calibration plot was  $y = 0.0628x + 0.0153$  with a correlation coefficient ( $R^2$ ) value as 0.9995. The regression equation obtained for pure Eze samples in USP acetate buffer (pH 4.5) from the corresponding eight-point calibration plot was  $y = 0.0618x + 0.1109$  with an  $R^2$  value as 0.9996. Similarly, the regression equation for pure Eze samples in distilled water (measured pH 6.8) from the corresponding eight-point calibration plot was  $y = 0.0629x + 0.0616$  with an  $R^2$  value as 0.9994. The UV-VIS method developed for pure Eze in each of the three media, 0.01 N HCl (pH 2), USP acetate buffer (pH 4.5) and distilled water (measured pH 6.8), was validated in terms of LOD, LOQ, precision and accuracy parameters. The validation parameters for the UV-VIS method developed for pure Eze using all the three media were presented in Table 5.1.

**Table 5.1. UV-VIS method validation parameters for pure Eze.**

| Parameters   | Results in different media (mean)       |                            |                      |
|--|---|----------------------------|----------------------|
|  | Distilled water<br>(measured pH<br>6.8) | Acetate buffer<br>(pH 4.5) | 0.01 N HCl<br>(pH 2) |
| $\lambda_{\max}$ (nm)  | 232                                     | 232                        | 232                  |
| Linearity range ( $\mu\text{g/mL}$ )                           | 2 – 30                                  | 2 – 30                     | 2 – 30               |
| LOD ( $\mu\text{g/mL}$ )                                       | 0.12                                    | 0.11                       | 0.12                 |
| LOQ ( $\mu\text{g/mL}$ )                                       | 0.35                                    | 0.32                       | 0.37                 |
| <b>Validation parameters at three different concentrations</b> |   |                            |                      |
| 2 $\mu\text{g/mL}$ (n = 3)                                     |   |                            |                      |
| Inter-day precision (% RSD); Accuracy (%)                      | 0.498; 100.5                            | 0.495; 101                 | 3.33; 99.83          |
| Intra-day precision (% RSD); Accuracy (%)                      | 0.495; 101                              | 0.761; 100.33              | 1.03; 101.33         |
| 4 $\mu\text{g/mL}$ (n = 3)                                     |   |                            |                      |
| Inter-day precision (% RSD); Accuracy (%)                      | 0.382; 99.92                            | 0.63; 100.17               | 1.71; 99.58          |
| Intra-day precision (% RSD); Accuracy (%)                      | 1.01; 100.08                            | 0.52; 100.08               | 2.31; 100.67         |
| 10 $\mu\text{g/mL}$ (n = 3)                                    |   |                            |                      |
| Inter-day precision (% RSD); Accuracy (%)                      | 0.2; 100.1                              | 0.15; 100.23               | 0.82; 100.2          |
| Intra-day precision (% RSD); Accuracy (%)                      | 0.208; 100.23                           | 0.1; 100.2                 | 0.73; 100.33         |

The LOD values were far lower than the required testing limits of the study which was quite desirable. The accuracy values of the standard Eze solutions represented by % Recovery were found to be consistent and efficient as all the results were within  $\pm 15\%$  of the actual values. The precision values represented by % RSD were also within the



specified limits of less than 15% for inter-day and intra-day precision [Bressolle et al., 1996, Jayasagar et al., 2002]. Thus, the UV analytical method developed was drug selective, accurate and precise. The same was applied to preformulation drug analysis, for estimating the drug content in prepared formulations and to study the solubility results and dissolution parameters of pure drug and formulations.

### 5.4.1.2 Phase solubility studies

The phase solubility diagram of Eze in the presence of NA/ND was presented in Figure 5.7. The results of our study indicated that the solubility of Eze increased with the increase in NA/ND concentration. However, the solubility of Eze increased non-linearly with a positive deviation in case of Eze-NA system. In the presence of ND, the solubility of Eze increased linearly. According to Higuchi and Connors [Higuchi and Connors, 1965], the phase solubility curves of Eze-NA and Eze-ND systems may be classified as  $A_P$  and  $A_L$  types, respectively. The results indicated the occurrence of Eze-coformer in the CoC lattices in the ratios, 1:2 and 1:1, in the systems, Eze-NA and Eze-ND, respectively. The ratios were further confirmed by constructing Job's plot (Figure 5.8). The K values were calculated from the straight line portions of the phase solubility curves. The slopes of the straight line portions of the phase solubility curves of Eze-NA and Eze-ND systems were 0.0013 and 0.0025, respectively and the K values calculated were  $260.34 \pm 5.67 \text{ M}^{-1}$  and  $501.25 \pm 7.98 \text{ M}^{-1}$ , respectively. Supramolecular complexes with association constant values in the range  $200 - 5000 \text{ M}^{-1}$  were said to illustrate improved dissolution and superior bioavailability [Patel et al., 2008]. To further narrow down, complexes with K values in the range of  $100 - 1000 \text{ M}^{-1}$  were believed to have wider industrial applications. While K values below  $100 \text{ M}^{-1}$  may indicate poor

association and instability of complexes, values above  $1000 \text{ M}^{-1}$  may affect the drug absorption adversely [Asbahr et al., 2009]. Both the CoCs presented reasonable stability and the higher K values with ND ( $p < 0.05$  in comparison to NA) may indicate plausibility of formation of more stable CoC assemblies with ND in comparison to NA.

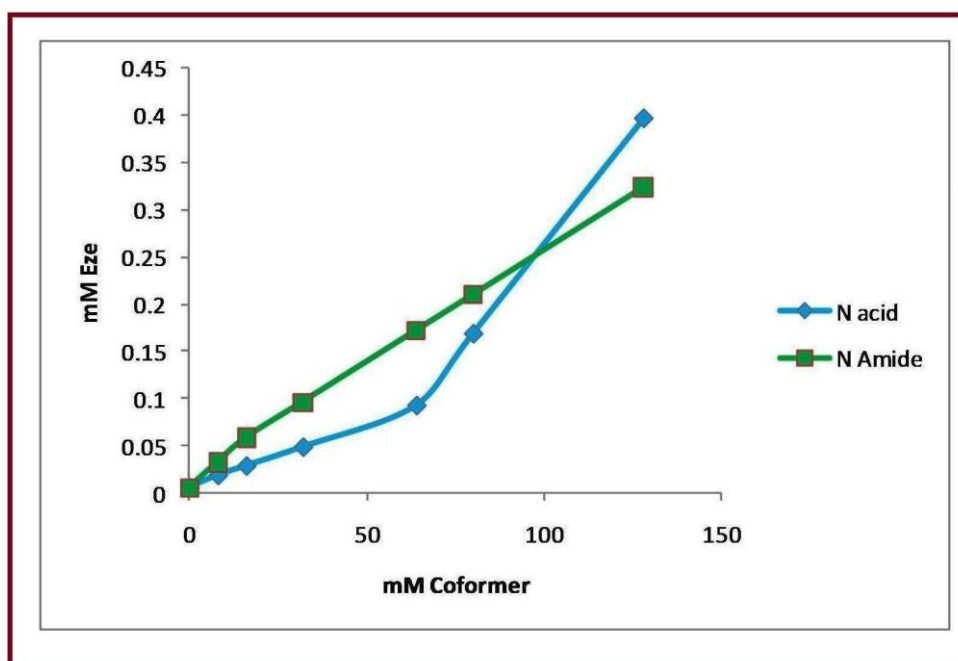


Figure 5.7. Phase solubility curves of liquid state CoC systems.

#### 5.4.1.3 Job's plot

The mole-ratio plots were constructed according to the continuous variation Job's method. Solutions containing varying mole fractions of Eze and NA/ND were prepared such that the total concentration of the two species in each of the solutions remained constant,  $0.005 \text{ mM}$ . The absorption values were measured at  $232 \text{ nm}$  (corresponding to Eze). The observed absorbance values of these solutions were different from the sum of the corresponding values of the respective individual components and the difference was calculated.

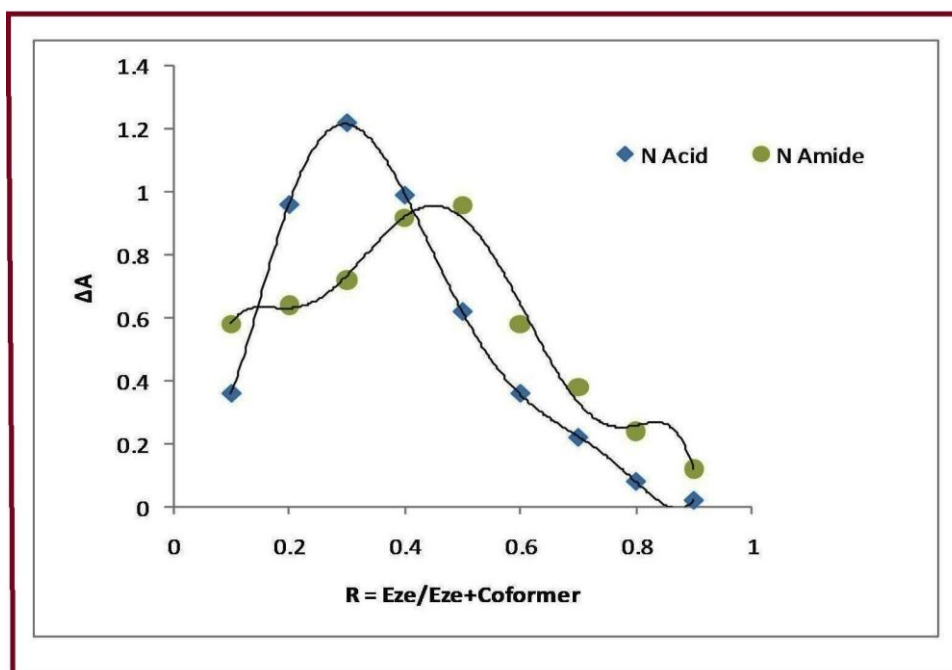


Figure 5.8. Job's plots of liquid state CoC systems.

This difference in absorbance was considered as an evidence for the CoC formation between Eze and NA/ND. As shown in Figure 5.8, the calculated absorbance difference was plotted against mole fraction of Eze,  $R$  ( $R = [\text{Eze}] / \{[\text{Eze}] + [\text{NA/ND}]\}$ ). For a fixed total concentration of two species, the CoC exists in its highest concentration at that point where the two species combine in the ratio in which they occur in the CoC. As depicted in Figure 5.8, significantly abrupt changes in the absorbance difference occurred at 0.33 mole fraction of Eze for Eze-NA system indicating that 1:2 is the optimal stoichiometric ratio of Eze-NA CoC. Similar studies showed 0.5 mole fraction of Eze and indicated 1:1 ratio of Eze-ND.

## 5.4.2 Characterization of Eze-NA and Eze-ND CoCs

### 5.4.2.1 Stoichiometric assay

#### 5.4.2.1.1 UV-VIS NA analysis – method development and validation

Analysis by UV–VIS spectrophotometry showed a characteristic peak corresponding to NA at 263.0 nm in distilled water. The standard calibration curve of NA was generated in distilled water, to quantify the samples. NA solutions were analyzed in the concentration range of 6 – 30 µg/mL. The UV-VIS spectral scan of pure NA in distilled water was shown in Figure 5.9 and the corresponding standard calibration curve was shown in Figure 5.10.

The regression equation obtained for standard NA solutions in distilled water from the corresponding six-point calibration plot was  $y = 0.0556x + 0.2014$  with an  $R^2$  value as 0.9997 where y represents the NA absorbance, x represents the concentration of NA, m is the slope of the plot, and c is the intercept. The standard calibration curve was found to be linear throughout the concentration range studied. The validation parameters for the UV-VIS method developed for pure NA in distilled water were presented in Table 5.2.

The LOD values were far lower than the required testing limits of the study which was quite desirable. The accuracy values of the standard NA solutions represented by % Recovery were found to be consistent and efficient as all the results were within  $\pm 15\%$  of the actual values. The precision values represented by % RSD were also within the specified limits of less than 15% for inter-day and intra-day precision [Bressolle et al., 1996; Jayasagar et al., 2002]. Thus, the UV analytical method developed was NA

selective, accurate and precise. The same was applied for the quantification of NA content in CoC formulation.

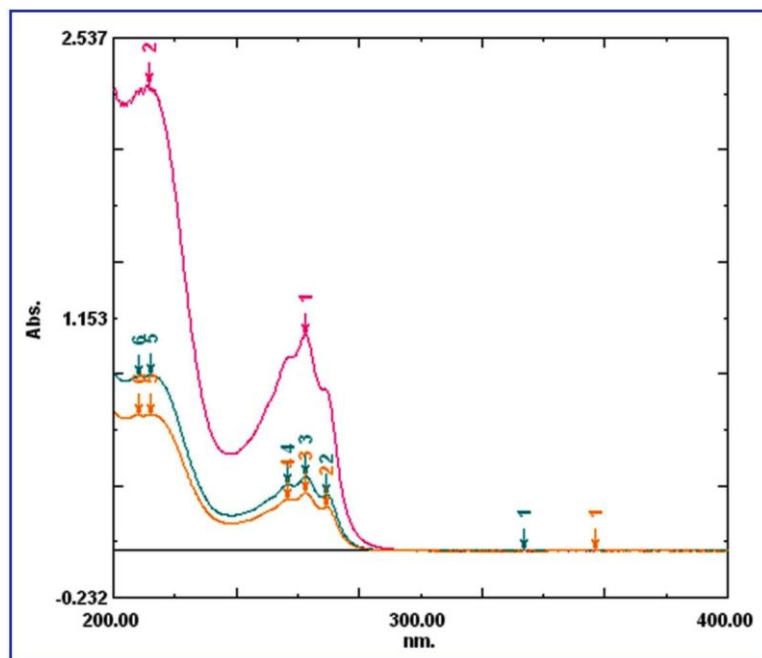


Figure 5.9. UV-VIS spectral scan of pure NA in distilled water.

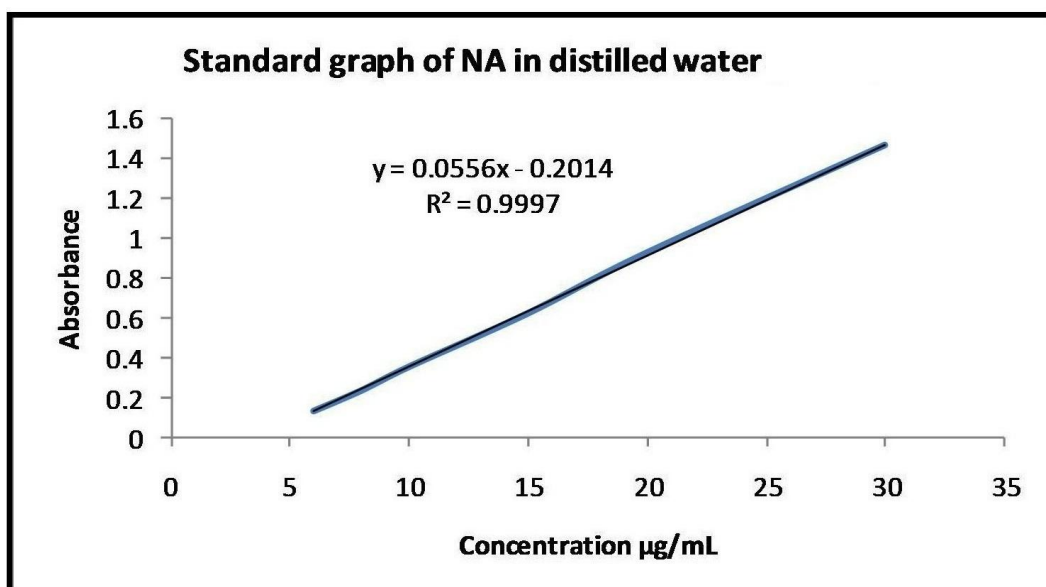


Figure 5.10. UV-VIS standard calibration curve of pure NA in distilled water.

Table 5.2. UV-VIS method validation parameters for pure NA.

| Parameters  | Results (mean) |
|---|----------------|
| $\lambda_{\max}$ (nm)   | 263            |
| Linearity range ( $\mu\text{g/mL}$ )  | 6 – 30         |
| LOD ( $\mu\text{g/mL}$ )  | 0.06           |
| LOQ ( $\mu\text{g/mL}$ )  | 0.18           |
| <b>Validation parameters at three different concentrations of stock solutions</b> |                |
| 6 $\mu\text{g/mL}$ (n = 3)  |                |
| Inter-day precision (% RSD); Recovery (%)   | 1.17; 99.67    |
| Intra-day precision (% RSD); Recovery (%)   | 0.35; 100.06   |
| 10 $\mu\text{g/mL}$ (n = 3)   |                |
| Inter-day precision (% RSD); Recovery (%)   | 0.2; 100.4     |
| Intra-day precision (% RSD); Recovery (%)   | 0.1; 100.2     |
| 20 $\mu\text{g/mL}$ (n = 3)   |                |
| Inter-day precision (% RSD); Recovery (%)   | 1.37; 101.27   |
| Intra-day precision (% RSD); Recovery (%)   | 0.85; 100.27   |

#### 5.4.2.1.2 UV-VIS ND analysis – method development and validation

Analysis by UV–VIS spectrophotometry showed a characteristic peak corresponding to ND at 262.0 nm in distilled water. Standard calibration curve of ND was generated in distilled water, to quantify the samples. ND solutions were analyzed in the concentration range of 4 – 20  $\mu\text{g/mL}$ . The UV-VIS spectral scan of pure NA in distilled water was shown in Figure 5.11 and the corresponding standard calibration curve was shown in Figure 5.12.

The regression equation obtained for standard ND solutions in distilled water from the corresponding six-point calibration plot was  $y = 0.1023x + 0.2549$  with an  $R^2$  value as 0.9992 where y represents the ND absorbance, x represents the concentration of ND, m

is the slope of the plot, and c is the intercept. The standard calibration curve was found to be linear throughout the concentration range studied.

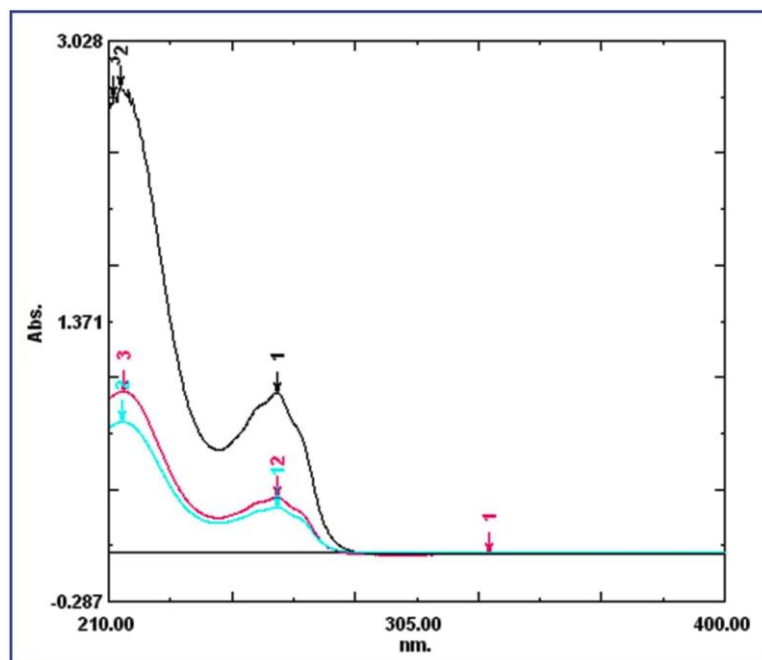


Figure 5.11. UV-VIS spectral scan of pure ND in distilled water.

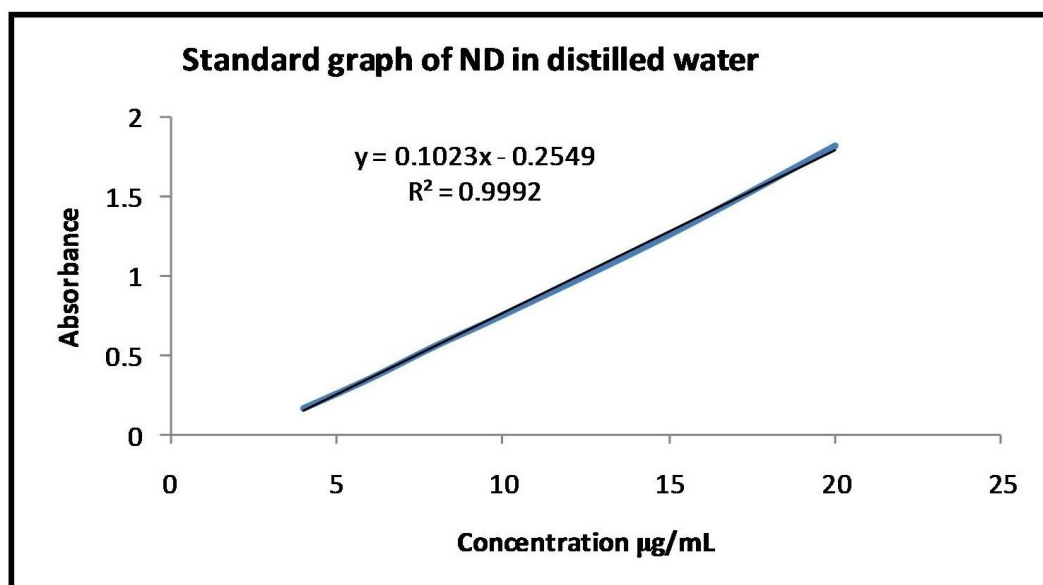


Figure 5.12. UV-VIS standard calibration curve of pure ND in distilled water.

The validation parameters for the UV-VIS method developed for pure ND in distilled water were presented in Table 5.3. The LOD values were far lower than the required testing limits of the study which was quite desirable. The accuracy values of the standard ND solutions represented by % Recovery were found to be consistent and efficient as all the results were within  $\pm 15\%$  of the actual values. The precision values represented by % RSD were also within the specified limits of less than 15% for inter-day and intra-day precision [Bressolle et al., 1996, Jayasagar et al., 2002]. Thus, the UV analytical method developed was ND selective, accurate and precise. The same was applied for the quantification of ND content in CoC formulation.

**Table 5.3. UV-VIS method validation parameters for pure ND.**

| Parameters  | Results (mean) |
|---|----------------|
| $\lambda_{\max}$ (nm)   | 262            |
| Linearity range ( $\mu\text{g/mL}$ )  | 4 – 20         |
| LOD ( $\mu\text{g/mL}$ )  | 0.07           |
| LOQ ( $\mu\text{g/mL}$ )  | 0.2            |
| <b>Validation parameters at three different concentrations of stock solutions</b> |                |
| 4 $\mu\text{g/mL}$ (n = 3)  |                |
| Inter-day precision (% RSD); Recovery (%)   | 1.71; 99.58    |
| Intra-day precision (% RSD); Recovery (%)   | 2.31; 100.67   |
| 10 $\mu\text{g/mL}$ (n = 3)   |                |
| Inter-day precision (% RSD); Recovery (%)   | 0.82; 100.2    |
| Intra-day precision (% RSD); Recovery (%)   | 0.73; 100.3    |
| 20 $\mu\text{g/mL}$ (n = 3)   |                |
| Inter-day precision (% RSD); Recovery (%)   | 0.77; 101.18   |
| Intra-day precision (% RSD); Recovery (%)   | 0.9; 100.18    |



#### **5.4.2.1.3 Stoichiometric assay results**

The CoCs in the present study were prepared by slow evaporation from a solution that contained stoichiometric amounts of the two components [drug and corresponding coformer (NA or ND)] of CoC. The stoichiometry was derived based on the preformulation studies where the construction of Job's plot suggested the occurrence of CoC components in the ratios (drug:coformer), 1:2 and 1:1, in Eze-NA and Eze-ND CoCs. The CoC stoichiometry was finally confirmed by assaying the contents of drug and coformer in the prepared CoC solid forms by employing UV-VIS spectrophotometric analysis.

The molar ratio percentages of Eze and NA in Eze-NA CoC were  $63.12 \pm 0.84\%$  and  $37.98 \pm 0.56\%$ , respectively. The preformulation studies suggested 1:2 ratio of Eze and NA in Eze-NA CoC and accordingly, solid form Eze-NA CoC was prepared by evaporation solution crystallization method. The stoichiometric assay results of solid form Eze-NA CoC confirmed 1:2 ration existence of Eze and NA in Eze-NA since theoretically, the molar ratio percentages of Eze and NA should be 62.44% and 37.56%.

The molar ratio percentages of Eze and ND in Eze-ND CoC were  $78.04 \pm 0.16\%$  and  $23.12 \pm 0.08\%$ , respectively. The preformulation studies suggested 1:1 ratio of Eze and ND in Eze-ND CoC and accordingly, solid form Eze-ND CoC was prepared by evaporation solution crystallization method. The stoichiometric assay results of solid form Eze-ND CoC confirmed 1:1 ration existence of Eze and ND in Eze-ND since theoretically, the molar ratio percentages of Eze and ND should be 77.024% and 22.976%.

### **5.4.2.2 Solid state characterization**

#### **5.4.2.2.1 FTIR studies**

Since the formation of a multicomponent CoC system is a result of intermolecular interactions between the starting components that exist in single crystalline state, IR spectroscopy could be powerful in detecting the CoC formation [Jayasankar et al., 2006]. The FTIR spectra of all the samples were shown in Figure 5.13. The FTIR peaks of the parent components were tabulated in Table 5.4. The FTIR spectrum of Eze-NA PM and Eze-ND PM were replicates of the pure Eze spectrum indicating that Eze was compatible with either of the coformers, NA or ND and that there was no chemical bonding or evidence of intermolecular interactions between Eze when it was compounded as a physical mixture with either NA or ND.

In case of both the CoCs, the Eze O–H peak presented bathochromic shift from 3267.52 to 3261.74  $\text{cm}^{-1}$ . Some of the principle absorption bands of coformers disappeared in the spectra of CoCs but none of the CoCs exhibited new peaks dismissing the possibility of formation of chemical bonds during cocrystallization. In both the CoC systems, modifications like broadening, attenuation and frequency shifts in the characteristic bands of the drug were noted. These results indicated that the vibrations and stretching of Eze molecule were restricted due to cocrystallization, which could have involved possible formation of hydrogen bonds between the drug and coformers. The participation of the O–H moieties of the drug molecule was clearly confirmed by FTIR.

In case of Eze-NA CoCs, a slight broadening of the O–H peak of Eze was observed, the carboxylic acid O–H stretching of NA at 3070.78  $\text{cm}^{-1}$  showed a hypsochromic shift to 3078.49  $\text{cm}^{-1}$ . The carboxylic acid C=O stretch of NA at 1710.92  $\text{cm}^{-1}$  was completely

disguised by the drug's C=O lactone stretch which showed a negligible bathochromic shift from 1718.7 to 1716.7  $\text{cm}^{-1}$ .

**Table 5.4. FTIR data table presenting characteristic peak assignments of parent compounds of CoCs.**

| <b>Parent compound</b> | <b>FTIR spectral bands and assignments</b>   |
|------------------------|--|
| <b>Eze</b>             | 3267.52 $\text{cm}^{-1}$ (broad stretching of intermolecular hydrogen bonded O–H), 2914.54 $\text{cm}^{-1}$ (stretching of aromatic C–H), 2958.9 $\text{cm}^{-1}$ (stretching of aliphatic C–H), 1886.44 $\text{cm}^{-1}$ (overtone band of lactone ring), 1718.69 $\text{cm}^{-1}$ (stretching of C=O of lactone ring), 1614.47 $\text{cm}^{-1}$ (vibration band of ring skeleton), 1510.31 $\text{cm}^{-1}$ (stretching of ring C–C), 1404.22 and 1444.73 $\text{cm}^{-1}$ (stretching of C–N), 1354.07 $\text{cm}^{-1}$ (bending of in plane O–H), 1273.06, 1220.98, and 1165.04 $\text{cm}^{-1}$ (stretching of C–F), 1066.67, and 1107.18 $\text{cm}^{-1}$ (stretching of C–O of secondary alcohol), 1016.52 $\text{cm}^{-1}$ (ring stretching of cyclobutanes), 941.29 $\text{cm}^{-1}$ (ring vibration of alkyl cyclobutanes), and 825.56 $\text{cm}^{-1}$ (ring vibration of para-disubstituted benzene) |
| <b>ND</b>              | 3363.97 and 3163.36 $\text{cm}^{-1}$ (asymmetric and symmetric N–H stretching vibrations), 1683.91 $\text{cm}^{-1}$ (amide C=O stretch), 1400.37, 1479.45 $\text{cm}^{-1}$ (stretching of aromatic ring C–C), 1346.36, 1612.54 $\text{cm}^{-1}$ (heteroaromatic ring stretch), and 779.27 $\text{cm}^{-1}$ (C–H out of plane bending vibrations of 3 substituted pyridine)   |
| <b>NA</b>              | 3070.78 $\text{cm}^{-1}$ (carboxylic acid O–H stretching vibrations), 1710.92 $\text{cm}^{-1}$ (carboxylic acid C=O stretch), 1417.73, 1494.88 $\text{cm}^{-1}$ (stretching of aromatic ring C–C), 1300.07, 1321.28, 1597.11 $\text{cm}^{-1}$ (heteroaromatic ring stretch), and 812.06 $\text{cm}^{-1}$ (C–H out of plane bending vibrations of 3 substituted pyridine)   |

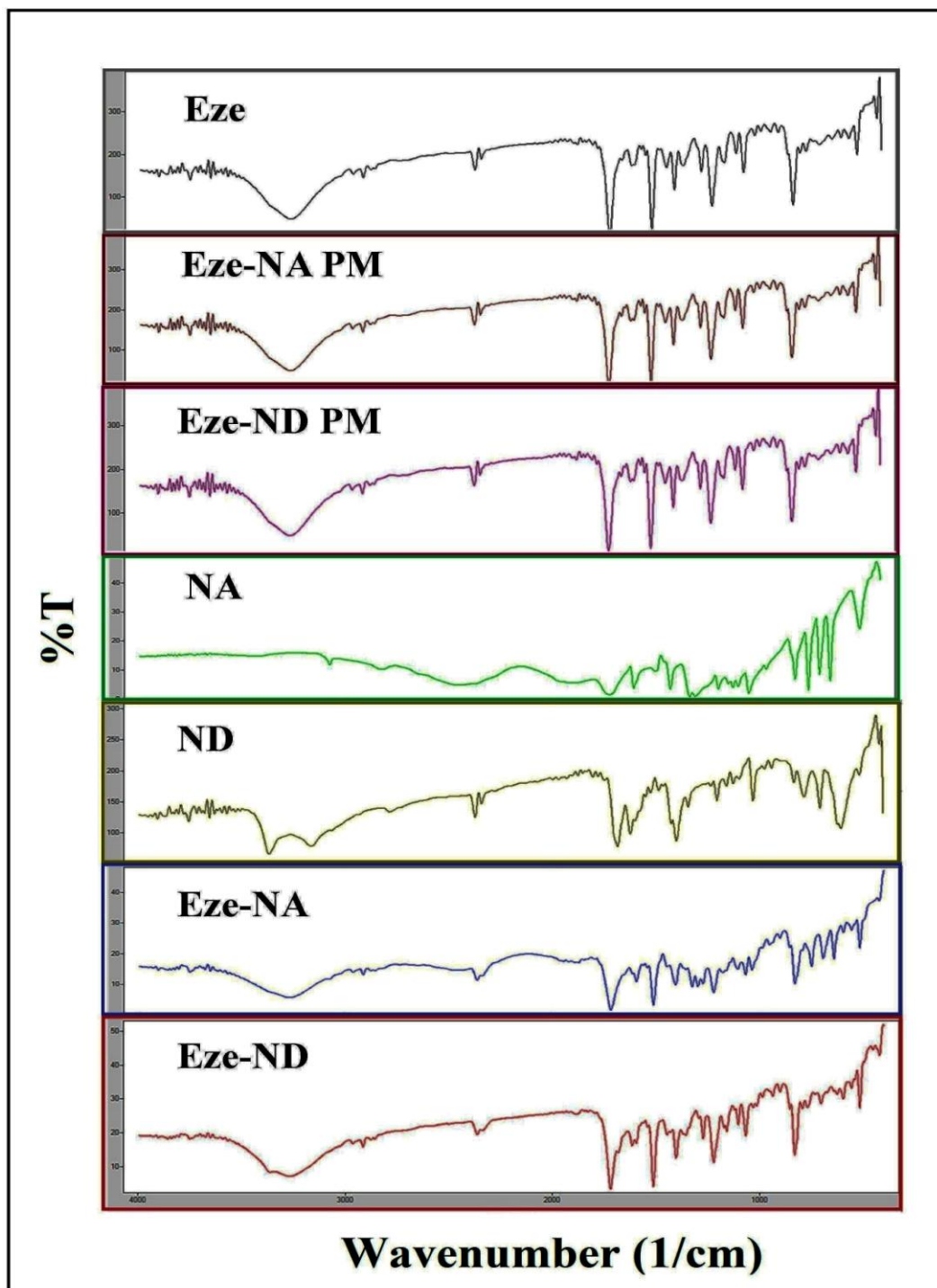


Figure 5.13. FTIR spectra of CoCs.

In case of Eze-ND CoCs, the shape of the O–H peak of Eze was altered by accommodating the asymmetric N–H stretch peak of ND. The peak corresponding to the ND's symmetric N–H stretching disappeared. The asymmetric N–H stretch at  $3363.97\text{ cm}^{-1}$  and amide C=O stretch at  $1683.91\text{ cm}^{-1}$  of ND showed hypsochromic and bathochromic shifts to  $3367.82$  and  $1680.05\text{ cm}^{-1}$ , respectively.

### 5.4.2.2.2 DSC

The thermal properties of pure drug, cofomers and CoCs were studied by DSC which detects phase transformations involving endothermic or exothermic changes. As shown in Figure 5.14, the DSC thermogram of Eze was characterized by a very sharp peak at  $163.56\text{ }^{\circ}\text{C}$ . The endotherms of NA and ND were observed at  $234.87\text{ }^{\circ}\text{C}$  and  $129.58\text{ }^{\circ}\text{C}$ , respectively.

The DSC thermograms of Eze-NA PM or Eze-ND PM retained the peaks corresponding to both of their respective parent components depicting the strong crystalline nature of drug and cofomer. In other words, the DSC thermograms of Eze-NA PM or Eze-ND PM were additive superpositions of the peaks of their corresponding raw materials. The DSC patterns of both the PMs confirmed that the cofomers did not alter the crystalline state of the drug when prepared as PMs. The melting endotherm of Eze-NA was noted at  $155.35\text{ }^{\circ}\text{C}$  and that of Eze-ND was seen at  $106.6\text{ }^{\circ}\text{C}$ .

Melting point is a fundamental physical property and is a measure of the energy required to break the attractive forces that hold a crystal together. Several factors such as strength of intermolecular interactions, chemical structure, molecular symmetry, crystal lattices, conformational degrees of freedom etc. contribute to melting point

[Katritzky et al., 2001]. In general, crystals containing stronger intermolecular bonding have greater molecular symmetry and higher melting point [Simperler et al., 2006]. CoCs are usually formed due to strong physical interactions between API and coformer. On account of strength and directionality, the most likely form of CoC interaction is formation of intermolecular hydrogen bonds between the polar functional groups of API and coformer [Gao et al., 2012]. Such bonds may result in moderate to complete alterations in the crystal habits of either API or coformer or both. Molecular arrangements occur to acquire a new crystal form of CoC because of which CoCs assume altered physical properties like melting point [Rodríguez-Hornedo et al., 2006]. Both the CoCs discovered in this work showed melting peaks different from their respective parent components.

A survey on 50 reported CoCs, conducted by Schultheiss and Newman, revealed that 50% of CoCs had melting points in between that of API and coformer, 40% had melting point lower than either of the parent components, 6% had higher and 4% had same melting point as either API or coformer [Schultheiss and Newman, 2009]. Both the coformers, NA and ND formed CoCs with lower melting points compared to either of the parent compounds. The order of appearance of melting point peaks for CoCs with NA was Eze-NA < Eze < NA and the order for CoCs with ND was Eze-ND < ND < Eze. CoCs presented characteristic sharp peaks distinguishable from either of the parent compounds and the peaks corresponding to the pure drug and coformer totally disappeared. These changes in the thermal behavior confirmed the formation of newly formed CoC lattice systems through intermolecular interactions between drug and NA/ND.

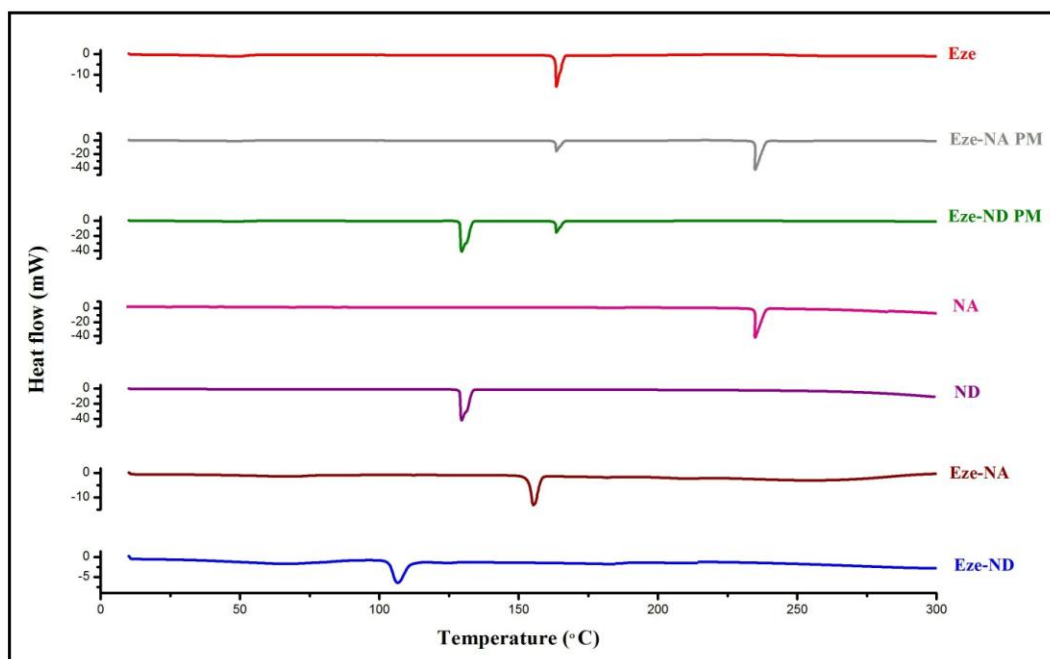


Figure 5.14. DSC thermograms of CoCs.

#### 5.4.2.2.3 PXRD

PXRD is a powerful technique to study the crystal habit modifications of solid substances and polymorphic changes in crystals. It serves to confirm the generation of new crystalline materials upon cocrystallization [Labhasetwar et al., 1993; Garekani et al., 2001]. Figure 5.15 shows X-ray diffractograms of all the samples. The spectra of pure drug and coformers showed characteristic sharp diffraction peaks confirming their crystalline nature. The PXRD peak assignments of parent compounds and CoCs have been listed in Table 5.5.

The PXRD peaks intensities of pure Eze, pure NA and pure ND were quite predominant with high intensity counts (cts). The PXRD patterns of Eze-NA PM or Eze-ND PM were additive superpositions of the patterns of their corresponding raw materials. The PXRD patterns of PMs retained the characteristic crystalline peaks and the

corresponding intensities pertaining to both of their respective parent components depicting the strong crystalline nature of Eze and either of the cofomers, NA or ND. The PXRD patterns of both the PMs confirmed that the cofomers did not alter the crystalline state of the drug in the PM form.

**Table 5.5. PXRD patterns of parent compounds and CoCs showing the peak heights in counts (cts) at various diffraction angles ( $2\theta^\circ$ ).**

| <u>Eze</u>      |                 | <u>ND</u>       |                 | <u>Eze-ND</u>   |                 | <u>NA</u>       |                 | <u>Eze-NA</u>   |                 |
|-----------------|-----------------|-----------------|-----------------|-----------------|-----------------|-----------------|-----------------|-----------------|-----------------|
| $2\theta^\circ$ | Height<br>(cts) | $2\theta^\circ$ | Height<br>(cts) | $2\theta^\circ$ | Height<br>(cts) | $2\theta^\circ$ | Height<br>(cts) | $2\theta^\circ$ | Height<br>(cts) |
| 18.6132         | 393.00          | 22.4065         | 427.95          | 14.4813         | 39.87           | 15.3537         | 322.38          | 18.6474         | 28.00           |
| 19.3288         | 692.00          | 24.9750         | 340.63          | 18.3488         | 57.53           | 20.2228         | 145.94          | 19.8078         | 46.00           |
| 21.7587         | 226.00          | 26.9494         | 972.01          | 19.1050         | 125.78          | 24.6914         | 230.65          | 23.2164         | 32.00           |
|                 |                 | 47.1194         | 303.25          | 22.5143         | 50.34           | 25.8552         | 293.10          | 24.3206         | 20.00           |
|                 |                 |                 |                 | 23.1044         | 54.36           | 26.7291         | 344.12          | 25.3586         | 26.00           |
|                 |                 |                 |                 | 25.0087         | 84.78           | 27.7987         | 201.88          | 26.3638         | 33.00           |
|                 |                 |                 |                 | 26.8201         | 57.79           |                 |                 | 26.8480         | 24.00           |
|                 |                 |                 |                 |                 |                 |                 |                 | 27.4099         | 33.00           |
|                 |                 |                 |                 |                 |                 |                 |                 | 29.2412         | 27.00           |
|                 |                 |                 |                 |                 |                 |                 |                 | 37.7727         | 15.00           |

Both the CoCs exhibited distinguished crystallographic structures and habits as compared to parent compounds. The peaks and the corresponding height recordings clearly distinguished the unique PXRD patterns of CoCs in comparison to pure Eze and cofomers. The diffraction angles recorded for CoCs were different from their respective parent crystals confirming their distinguished internal structure and crystal



habit. For the  $2\theta^\circ$  peaks of CoCs that overlapped with those of their corresponding parent crystals, the intensities were significantly reduced (confirmed by peak heights measured in cts). These observations suggest the molecular arrangements underwent by the respective parent crystals to generate new crystal forms. DSC analysis also confirmed the distinguished melting peaks exhibited by the CoCs as compared to their respective parent crystals. The formation of new CoCs has been established by both DSC and PXRD analysis.

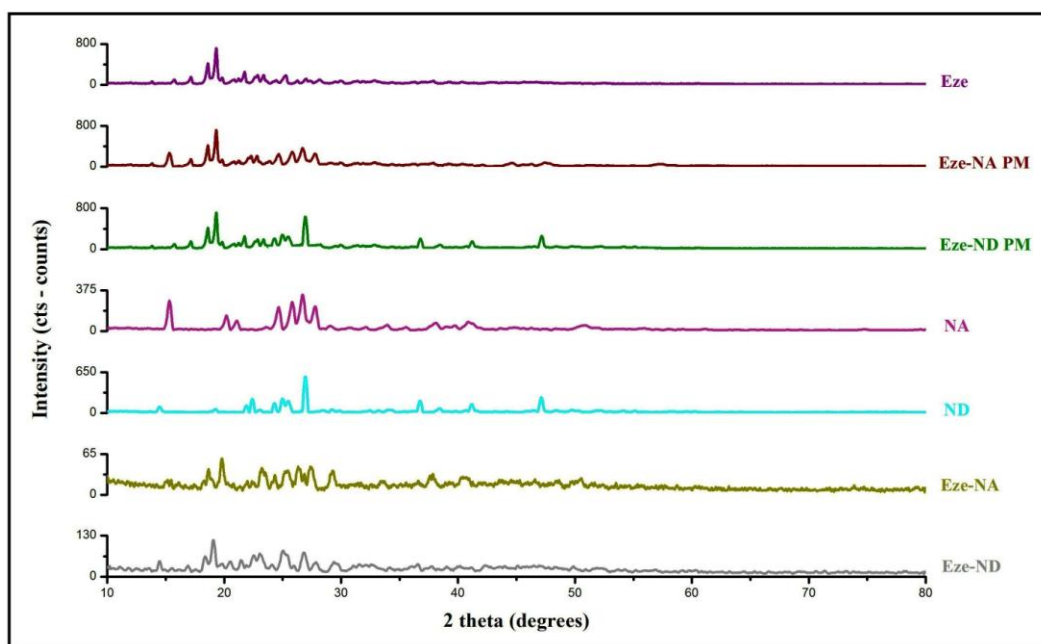
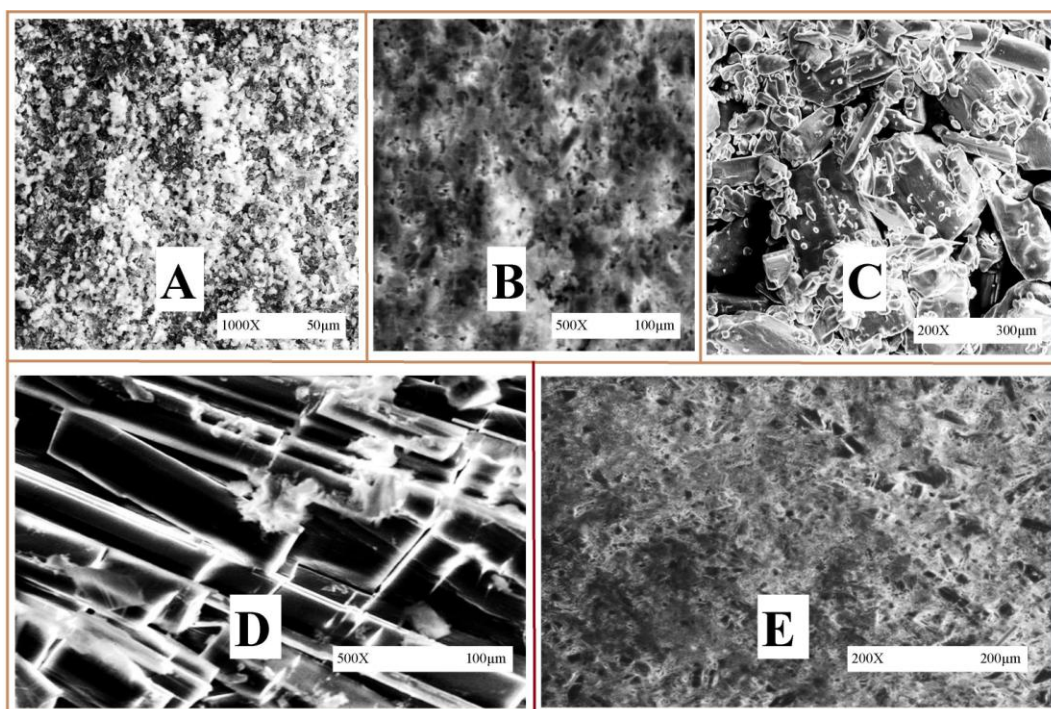


Figure 5.15. X-ray diffractograms of CoCs.

#### 5.4.2.2.4 SEM

The SEM images of all the samples were shown in Figure 5.16. Pure Eze existed as small stone shaped particles, NA existed as pebble shaped particles and ND appeared as small and large block shaped particles. The stone shaped drug appearance was completely transformed on cocrystallization.

CoCs appeared as glossy crystals with shining smooth surface indicating the disappearance of the original morphology of their respective parent components and confirmed the formation of new crystal habits. Eze-NA CoCs appeared as smooth surfaced transparent rod shaped crystals and Eze-ND CoCs looked like slightly rough surfaced irregular shaped flakes. The photomicrographs suggested formation of new solid state crystal forms of Eze with both the employed cofomers. CoCs showed altered morphological properties, with differentiable particle shape, size and surface characteristics when compared to their respective parent crystals.



**Figure 5.16. SEM photomicrographs of (A) Eze; (B) NA; (C) ND; (D) Eze-NA; (E) Eze-ND.**

#### 5.4.2.2.5 TGA

The TGA graphs of both the CoCs were presented in Figure 5.17. The changes in the weight of CoCs with change in temperature have been noted.

No weight loss was depicted by either of the CoCs ahead of their respective melting points indicating absence of any weight loss corresponding to residual solvents. This observation suggested that the formed CoCs were not CoC solvates [Gao et al., 2012; Kilinkissa, 2014]. The weight loss observed in the TGA graph of both the CoCs beyond the melting points of CoCs may be related to degradation of parent compounds.

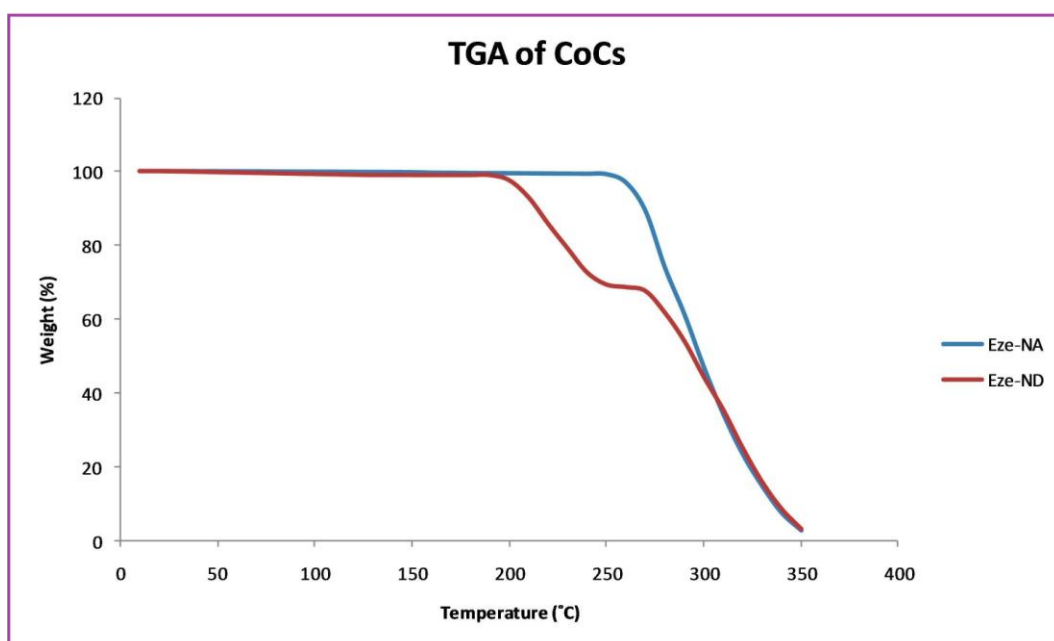


Figure 5.17. TGA graphs of CoCs.

#### 5.4.2.3 Flow properties

Since literature suggests that CoCs are likely to improve the flow properties of parent drug molecules [Gagniere et al., 2009a; Mulye et al., 2012], a study of flow characteristics of the CoCs was made part of this section of research work. The flow

properties of pure drug and CoCs were presented in Table 5.6. AR, CI and HR were the flow properties studied and these properties of CoCs were compared to those of pure drug. Both the CoCs presented significantly superior flow properties in comparison to pure Eze ( $p < 0.05$ ) while the difference in the flow characteristics between Eze-NA and Eze-ND CoCs was insignificant ( $p > 0.05$ ). The improved flow properties of CoCs may be attributed to the altered particle size, shape and crystal habitat achieved upon cocrystallization [Mulye et al., 2012]. Pure Eze was stone shaped with size as small as 2-3  $\mu\text{m}$  and both the CoCs assumed an increase in size (almost five to tenfold). CoCs were rod or flaky shaped and assumed larger particle size as shown in SEM photographs. Smaller particles may exhibit higher cohesive forces which might result in poor flow characteristics. These cohesive forces might have been reduced with the increase in particle size and shape attained by CoCs which resulted in their improved flow properties [Aulton, 1998; Subrahmanyam, 2000].

**Table 5.6. Flow properties of parent compounds and CoCs. Data shown as Mean $\pm$ SD (n = 3).**

| System    | Angle of repose ( $\theta^\circ$ ) | Hausner's ratio   | Compressibility index (%) |
|-----------|------------------------------------|-------------------|---------------------------|
| Pure drug | 37.28 $\pm$ 0.88                   | 1.288 $\pm$ 0.010 | 22.38 $\pm$ 0.782         |
| Eze-ND    | 26.26 $\pm$ 1.01                   | 1.137 $\pm$ 0.011 | 12.06 $\pm$ 0.841         |
| Eze-NA    | 26.32 $\pm$ 0.69                   | 1.135 $\pm$ 0.001 | 11.93 $\pm$ 0.084         |

#### 5.4.2.4 Drug content

The drug content analysis was performed in triplicate and averaged. The percentages of drug content in Eze-NA and Eze-ND were found to be 99.7 $\pm$ 1.26% w/w and

101.26±2.18% w/w, respectively. The results indicated that the drug was uniformly present in both the CoC systems.

#### 5.4.2.5 Saturation aqueous solubility studies

Two independent factors that determine solubility are the strength of crystal lattice (inversely) and the solvent affinity of CoC components (directly). CoCs are capable of influencing both these factors [Thakuria et al., 2013]. Accordingly, the solubility of Eze was improved by 5 – 10 folds upon cocrystallization. The aqueous solubilities were significantly increased in the order: Eze < Eze-NA < Eze-ND ( $p < 0.05$  for each comparison). The solubility results were given in Table 5.7.

**Table 5.7. Saturation solubility (n = 3) and dissolution (n = 6) results of pure Eze and CoCs. Data shown as Mean±SD.**

| System    | Saturation aqueous solubility (µg/mL) | t <sub>80%</sub> (min)     | t <sub>90%</sub> (min)    | DE <sub>120</sub> (%)         |
|-----------|---------------------------------------|----------------------------|---------------------------|-------------------------------|
| Pure drug | 1.99±0.62                             | Not Achieved               | Not Achieved              | 24.91±1.46                    |
| Eze-NA PM | Not applicable                        | Not Achieved               | Not Achieved              | 25.4±1.92                     |
| Eze-ND PM | Not applicable                        | Not Achieved               | Not Achieved              | 26.5±1.88                     |
| Eze-NA    | 9.19±1.18 <sup>a*</sup>               | 52.9±2.87                  | 73.5±3.17                 | 74.65±3.05 <sup>####</sup>    |
| Eze-ND    | 20.32±3.85 <sup>a***, b**</sup>       | 14.13±0.93 <sup>b***</sup> | 24.4±1.08 <sup>b***</sup> | 91.3±4.17 <sup>\$\$\$\$</sup> |

Symbols and statistical representations = \*\*\* $p < 0.001$ , \*\* $p < 0.01$  and \* $p < 0.05$ ; a = compared to pure Eze; b = compared to Eze-NA; @ = compared to pure Eze and Eze-NA; # = compared to pure Eze, Eze-NA PM and Eze-ND PM; \$ = compared to pure Eze, Eze-NA PM, Eze-ND PM and Eze-NA (One way ANOVA followed by Tukey's post hoc test).

As already discussed, the intermolecular hydrogen bonds serve to assemble the CoC components and generate a unique CoC form because of which CoCs assume altered physical properties like melting point and/ or solubility [Katritzky et al., 2001; Simperler et al., 2006; Rodríguez-Hornedo et al., 2006]. PXRD graphs confirmed the altered crystal habits of both the CoCs and DSC thermograms clearly indicated the distinguished melting peaks of both the CoCs indicating the strength of newly formed hydrogen bonds between API and coformers.

Literature suggests existence of correlation between the melting point of a CoC and its solubility. CoCs with higher melting point tend to have lower solubility and vice-versa [Stanton and Bak, 2008; Schultheiss and Newman, 2009]. This conversation has been documented by the authors of the AMG 517 CoCs study wherein the authors constructed a correlation plot between the Log of maximum solubility ( $\text{Log } S_{\text{max}}$ ) and melting point of nine CoCs and identified highest interdependence of 55% between the two parameters [Stanton and Bak, 2008]. The saturation solubility results obtained in this study were in agreement with the literature reports. Eze-NA CoCs presented higher melting point at 155.35 °C and Eze-ND CoCs presented melting point at lower temperature, 106.6 °C. Accordingly, the aqueous solubility result of Eze-NA was markedly lower in comparison to Eze-ND. Apart from lower melting point, higher hydrophilicity of coformer ND and the altered crystal size and shape of Eze-ND might have also contributed to its higher solubility.

### **5.4.2.6 Dissolution**

Though Eze contains ionisable groups [Figure 2.17], literature suggests that the drug essentially shows a pH independent solubility characteristic across the GIT pH range.

Thus, pH-based strategies to improve the solubility/dissolution characteristics (e.g. salts, addition of pH modifiers) were not a first-line option for a drug like Eze [Taupitz et al., 2013]. For the same reason, the formulations in this study were optimized by studying their dissolution in just one pH media, the USP acetate buffer medium of pH 4.5, containing 0.45% w/v sodium lauryl sulphate, as per by the USFDA Dissolution Methods Database guide for Eze.

Dissolution testing enables investigation of solubility of drug in its solid state allowing assumptions to be made with respect to the possible *in-vivo* behavior of the formulations [Childs et al., 2013]. The dissolution efficiency (DE) at 120 min,  $t_{80\%}$  and  $t_{90\%}$  values were calculated for pure Eze, PMs and CoCs, and tabulated in Table 5.7. The dissolution profiles of all the systems were presented in Figure 5.18.

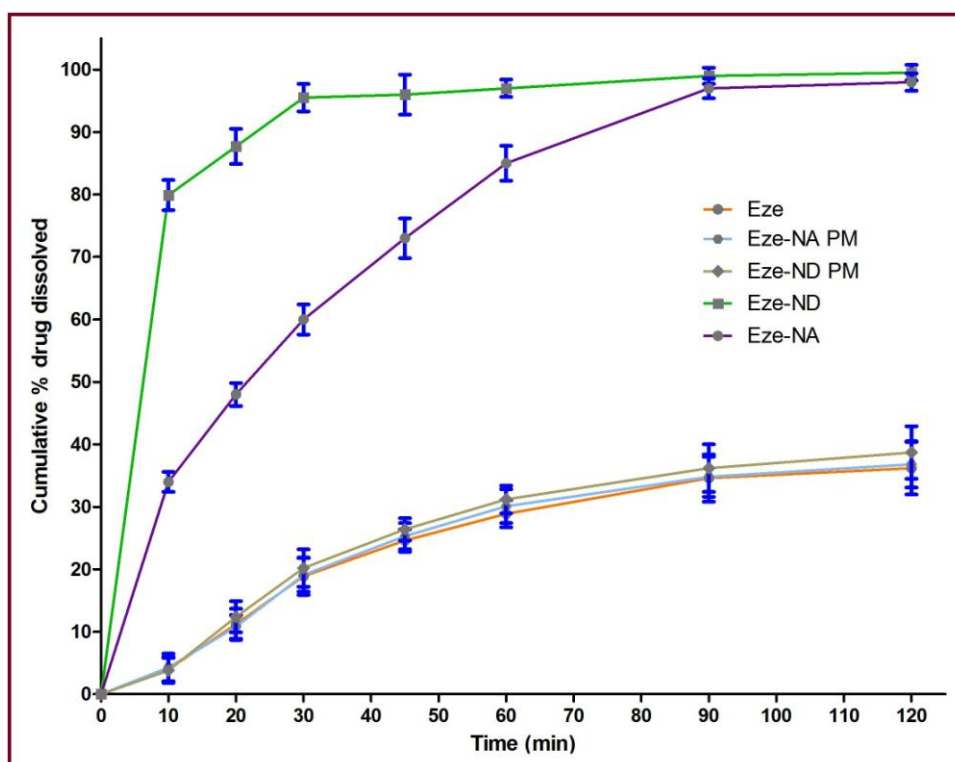


Figure 5.18. Dissolution profiles of pure drug, PMs, Eze-NA, and Eze-ND (vertical bars represent SD, n = 6).



The findings showed that pure Eze obviously presented the lowest dissolution rate because of its low solubility and the  $DE_{120}$  (%) was greater for both the CoCs in comparison to pure Eze ( $p < 0.05$ ). Similarly, the  $DE_{120}$  (%) was greater for both the CoCs in comparison to either of the PMs ( $p < 0.05$ ). Pure drug did not dissolve more than  $36.2 \pm 4.2\%$ , during 120 min dissolution study. The PMs also presented a low dissolution rate similar to pure drug ( $p > 0.05$ ) as pure Eze  $\approx$  Eze-NA PM  $\approx$  Eze-ND PM, and none achieved  $t_{80\%}$  and  $t_{90\%}$  during the study period.

$DE_{120}$  was improved by 3 – 4 folds on cocrystallization as compared to pure Eze. The use of a cofomer with higher water solubility resulted in CoCs with higher water solubility and dissolution rate when compared to pure drug [Alhalaweh et al., 2012; Shimpi et al., 2014]. Accordingly, both the CoCs showed better solubility and dissolution compared to Eze and the behavior of Eze-ND CoCs was superior to Eze-NA CoCs due to higher water solubility of ND. The  $DE_{120}$ ,  $t_{80\%}$  and  $t_{90\%}$  values of Eze-ND were significantly higher compared to Eze-NA ( $p < 0.05$ ).

The superior dissolution of Eze from CoCs could be the result of altered crystal assembly, size, shape and habit of CoCs. The improved solubility may also have contributed to rapid dissolution of drug from CoCs. Fair stability or association constants of CoCs, stability of CoCs against transformation to individual crystals and prevention of formation of low soluble hydrate form of Eze, might also be considered as possible reasons for enhanced dissolution performance of CoCs [Yadav et al., 2010; Mulye et al., 2012]. Better dissolution from Eze-ND could be the result of linear phase solubility relation between Eze and ND ( $A_L$  curve) as opposed to the  $A_P$  pattern relation between Eze and NA. Lack of precipitation problem on dilution of supramolecular



complexes is a reported advantage with  $A_L$  patterned phase solubility curves [Stella and Rajewski, 1997].

#### 5.4.2.7 Stability

The stability of the optimized CoCs was studied at  $30\pm 2$  °C/ $70\pm 5\%$  RH for 6 months. The samples withdrawn after 6 months were analysed and the changes in the drug content, solubility and dissolution were noted at the end of 6 months.

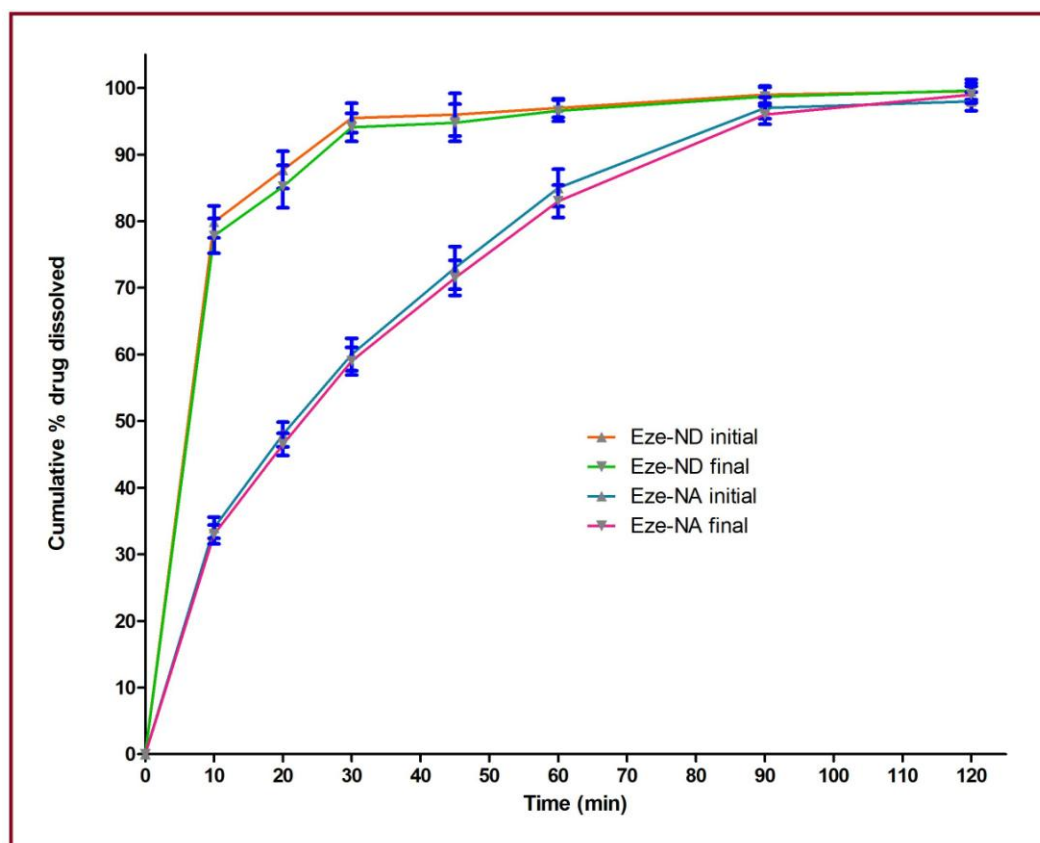


Figure 5.19. Dissolution profiles of Eze-NA and Eze-ND from stability studies (vertical bars represent SD, n = 6).

**Table 5.8. Stability study observations of optimized CoCs. Data shown as Mean±SD and n = 3 (n = 6 for dissolution data).**

| Tests  | Properties before stability storage studies |   | 30±2 °C/70±5% RH storage evaluation after 6 months |   |            |
|--|---|---|--|---|------------|
|  | Eze-NA (initial)                            | Eze-ND (initial)                            | Eze-NA (final)                                     | Eze-ND (final)                              |            |
| <b>Description</b>   | Fine cream crystals                         | Fine white crystals                         | Complies   | Complies                                    |            |
| <b>Stoichiometry assay by UV (mole ratio %)</b>              | 63.12±0.84%<br>Eze and<br>37.98±0.56%<br>NA | 78.04±0.16%<br>Eze and<br>23.12±0.08%<br>ND | 63.08±1.02%<br>Eze and<br>38.14±0.28%<br>NA        | 77.98±0.04%<br>Eze and<br>23.02±0.12%<br>ND |            |
| <b>Drug content by UV (%)</b>                                | 99.7±1.26                                   | 101.26±2.18                                 | 99.2±1.4   | 100.88±2.26                                 |            |
| <b>Saturation aqueous solubility (10<sup>-3</sup> mg/mL)</b> | 9.19±1.18                                   | 20.32±3.85                                  | 9.12±1.22  | 20.14±3.68                                  |            |
| <b>Dissolution by UV</b>                                     | <b>DE<sub>120</sub> (%)</b>                 | 74.65±3.05                                  | 91.3±4.17  | 73.65±2.88                                  | 90.5±3.02  |
|  | <b>t<sub>80%</sub> (min)</b>                | 52.9±2.87                                   | 14.13±0.93   | 54.1±2.92                                   | 14.53±1.12 |
|  | <b>t<sub>90%</sub> (min)</b>                | 73.5±3.17                                   | 24.4±1.08  | 74.72±3.42                                  | 25±1.66    |

The results suggested that both the CoCs, Eze-NA and Eze-ND, were stable with statistically insignificant changes in the studied properties. There was no visible change in the appearance of the CoCs even after 6 months of stability testing. The drug content results indicated that there was no significant change in the Eze content after 6 months when compared with the initial value. Similarly, no statistically significant variation

was observed in the solubility results and dissolution test parameters during the stability testing period. The dissolution study profiles following stability study were shown in Figure 5.19. The CoCs maintained their stability for the period of 6 months suggesting that the storage of CoCs at room temperature may be considered acceptable. The stability study results and observations were given in Table 5.8.

### 5.4.2.8 *In-vivo* preclinical pharmacokinetic study

#### 5.4.2.8.1 HPLC-UV plasma drug analysis – method development and validation

HPLC-UV method was developed with an aim to serve the purpose of bioanalysis of plasma drug samples. The developed HPLC-UV method was used for drug estimation in rat plasma during animal pharmacokinetic studies of pure drug and formulations. Eze solutions were analyzed in the concentration range of 100–8000 ng/mL. Two sets of standard calibration curves of Eze were generated for drug quantification using a) standard analytical drug samples (in mobile phase and unextracted); and b) standard bioanalytical plasma spiked drug + IS samples (extracted and reconstituted in mobile phase).

Isocratic separation was performed by using mobile phase of 60:40 v/v acetonitrile and 0.1 M ammonium acetate aqueous solution. Acetonitrile was used as mobile phase solvent due to its low viscosity (0.37 cp), high resolution and better separation efficiency. Eze analysis by HPLC was facilitated using UV detector at 232 nm wavelength (characteristic UV-VIS  $\lambda_{\max}$  of Eze). As mentioned, standard calibration curves of pure Eze solutions (unextracted analytical samples) and spiked plasma drug solutions (extracted bioanalytical plasma drug samples) were constructed in the range of

100 – 8000 ng/mL. The standard calibration curve of Eze was initially plotted using pure drug solutions, validated and the plasma drug EE of the developed analytical HPLC-UV method was determined. Plasma Eze EE was calculated by comparing the peak areas of spiked plasma samples (n = 3) with those of standard unextracted analytical solutions at the same concentration. A little drug loss occurred during the extraction process but the EE of analytical HPLC-UV method established the suitability of developing bioanalytical HPLC-UV method for plasma Eze analysis. As the EE confirmed good consistency and efficiency of the developed analytical method, standard calibration curve of standard plasma spiked Eze solutions was exercised. The chromatograms of pure drug sample, blank plasma and spiked plasma drug sample were shown in Figure 5.20. (the Figure shows the elution up to 6 min to cover the drug peaks).

The HPLC (Shimadzu Corporation, koyoto, Japan) analyses of analytical and bioanalytical samples were carried out using UV detector at 232 nm wavelength, corresponding to UV  $\lambda_{\text{max}}$  of Eze. Retention times noted were,  $5.491 \pm 0.048$  min (n = 6) and  $5.495 \pm 0.062$  min (n = 6), respectively, for pure drug samples and spiked plasma drug samples. No other plasma components were eluted at the retention time of Eze. IS was eluted at  $8.09 \pm 0.086$  min (n = 6).

Standard calibration curves of pure analytical Eze solutions (unextracted samples) and spiked plasma drug solutions (extracted bioanalytical samples) were generated in the concentration range of 100 – 8000 ng/mL as shown in Figure 5.21 and 5.22.

The regression equation ( $y = mx + c$ ) obtained for standard analytical Eze samples, from the corresponding eight-point calibration plot was  $y = 129.07x + 1388.5$  with an  $R^2$  value as 0.9999 where y represents the Eze peak area, x represents the concentration of

Eze,  $m$  is the slope of the plot, and  $c$  is the intercept. The standard calibration curve was found to be linear throughout the concentration range studied.

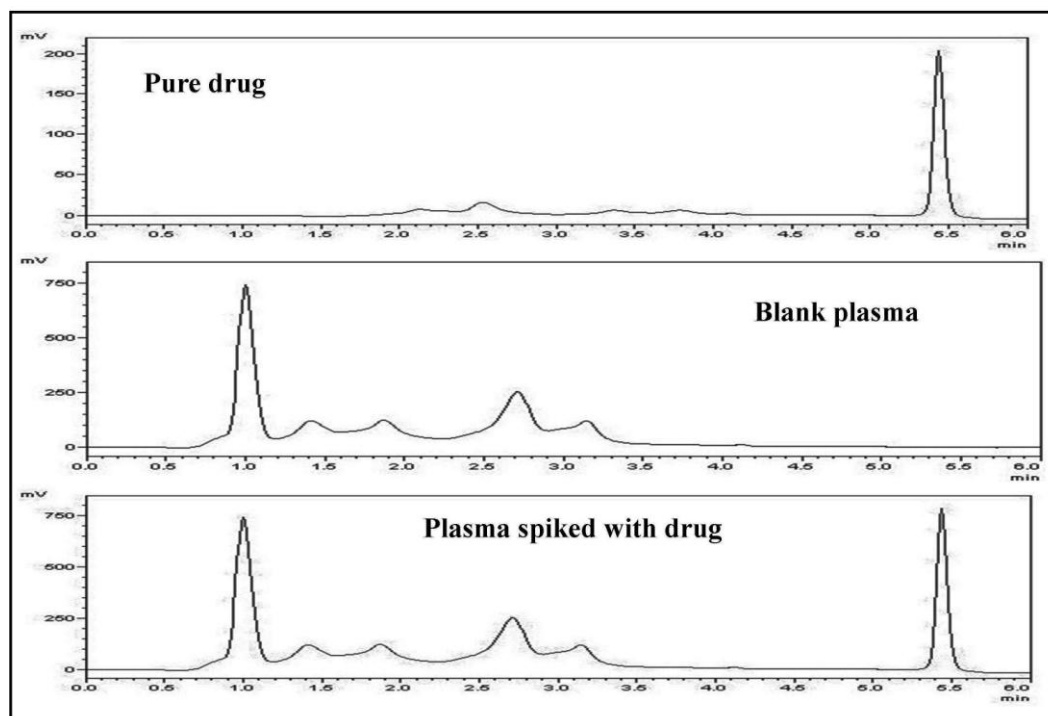


**Figure 5.20. HPLC chromatograms of pure Eze (analytical) sample, blank plasma and plasma spiked Eze (bioanalytical) sample.**

The regression equation ( $y = mx + c$ ) obtained for standard bioanalytical - spiked rat plasma Eze samples, from the corresponding eight-point calibration plot was  $y = 0.0162x + 0.047$  with an  $R^2$  value as 0.9999 where  $y$  represents the Eze:IS peak-area ratio,  $x$  represents the concentration of Eze,  $m$  is the slope of the plot, and  $c$  is the intercept. The standard calibration curve was found to be linear throughout the concentration range studied.

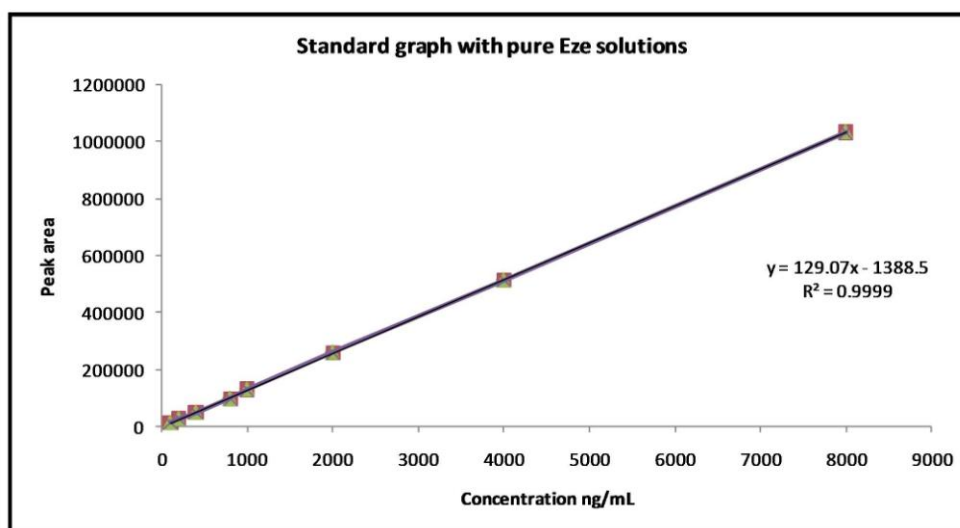


Figure 5.21. HPLC-UV standard calibration curve of pure Eze analytical samples.

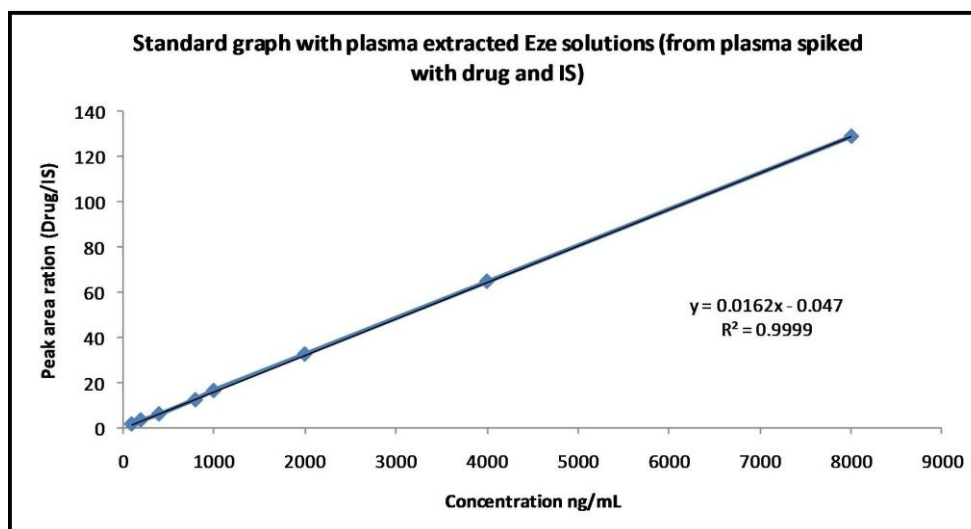


Figure 5.22. HPLC-UV standard calibration curve of plasma spiked Eze bioanalytical samples.

Both analytical and bioanalytical methods were validated in terms of linearity, LOD, LOQ, precision (inter day and intraday variation) and accuracy. For intra-day precision and accuracy, three replicate drug samples at each concentration were assayed on the

same day, at three different time points. The inter-day precision and accuracy were evaluated on three different days. The results are summarized in Table 5.9.

**Table 5.9. HPLC-UV method validation parameters for analytical and bioanalytical Eze samples.**

| Parameters   | Results (mean)          |                       |
|--|-------------------------|-----------------------|
|  | Pure drug (unextracted) | Plasma extracted drug |
| $\lambda_{\max}$ (nm) and Retention time (min)   | 232 and 5.491           | 232 and 5.495         |
| Linearity range (ng/mL)  | 100 – 8000              | 100 – 8000            |
| LOD (ng/mL)  | 1.04                    | 5.71                  |
| LOQ (ng/mL)  | 3.14                    | 17.32                 |
| <b>Validation parameters at three different concentrations of stock solutions</b>            |                         |                       |
| 200 ng/mL (n = 3)  |                         |                       |
| Inter-day precision (% RSD); Accuracy (%)  | 4.88; 100.2             | 4.88; 100.2           |
| Intra-day precision (% RSD); Accuracy (%)  | 5.04; 101               | 4.86; 100.2           |
| 400 ng/mL (n = 3)  |                         |                       |
| Inter-day precision (% RSD); Accuracy (%)  | 3.84; 98.5              | 3.84; 98.5            |
| Intra-day precision (% RSD); Accuracy (%)  | 5.21; 99.2              | 2.78; 99.3            |
| 1000 ng/mL (n = 3)   |                         |                       |
| Inter-day precision (% RSD); Accuracy (%)  | 2.52; 99.9              | 2.08; 100.4           |
| Intra-day precision (% RSD); Accuracy (%)  | 2.65; 100.1             | 2.08; 100.4           |
| <b>Extraction efficiency (EE) at three different concentrations of spiked plasma samples</b> |                         |                       |
| Concentration (ng/mL) / Recovery (%)   | Inter-day (%)           | Intra-day (%)         |
| 200 ng/mL (n = 3)  | 89.27                   | 88.23                 |
| 400 ng/mL (n = 3)  | 90.44                   | 88.63                 |
| 1000 ng/mL (n = 3)   | 90.22                   | 90.2                  |
| <b>Mean EE from plasma</b>   | 89.02                   | 89.98                 |

The linearity range of both, the analytical and bioanalytical HPLC-UV standard calibration plots, was found to be suitable for plasma Eze analysis. The LOD values were far lower than the required testing limits of the study which was quite desirable. The accuracy values represented by % Recovery were found to be consistent and efficient as all the results were within  $\pm 15\%$  of the actual values. The precision values represented by % RSD were also within the specified limits of less than 15% for inter-day and intra-day precision [Bressolle et al., 1996, Jayasagar et al., 2002].

To summarize, an analytical HPLC-UV method was initially developed by constructing standard calibration curve of standard unextracted analytical drug solutions, validated and the plasma drug EE of the method was determined. As the EE confirmed good consistency and efficiency of the developed analytical method, bioanalytical HPLC-UV method was subsequently developed and validated. Accordingly, standard calibration curve of standard extracted bioanalytical plasma spiked Eze solutions was exercised. Thus developed bioanalytical HPLC-UV method was drug selective, accurate and precise. This method was employed for *in-vivo* preclinical plasma drug analysis following oral administration of pure drug or formulations to lab animals (rats) to study single dose pharmacokinetics. Eze in rat plasma was conveniently detected and quantified by using this bioanalytical HPLC-UV method.

### 5.4.2.8.2 Pharmacokinetic parameters

The pharmacokinetic parameters were determined using Kinetica 5.0 pharmacokinetic software (Trial version, PK-PD analysis, Thermofischer) and Graphpad Prism software (version 5.03, GraphPad Software, USA). The plasma profiles of total Eze quantified in



adult male Albino Wistar rats following single dose oral administration of pure drug suspension, Eze-NA and Eze-ND were reported in Table 5.10.

The peak plasma concentration ( $C_{max}$ ) and the time to attain  $C_{max}$ ,  $T_{max}$ , were recorded directly from the plasma concentration – time curve. The area under the plasma concentration – time curve was determined by trapezoidal method. It was noticed that the plasma concentration time profile of Eze for CoCs showed improved drug absorption than the simple drug suspension.

**Table 5.10. Pharmacokinetic parameters derived for pure Eze and CoCs (n = 6). Data shown as Mean±SD.**

| Parameter/Treatment   | Pure drug        | Eze-NA           | Eze-ND                           |
|---|------------------|------------------|----------------------------------|
| $T_{max}$ (h)   | 2±0.00           | 2±0.00           | 1±0.00                           |
| $C_{max}$ (ng/mL)   | 1912±195.92      | 2212±235.68      | 4173±396.92 <sup>@***</sup>      |
| AUC <sub>0-24h</sub> (ng. h/mL)   | 17848±1306.54    | 19152±1369.96    | 29263±1438.52                    |
| AUC <sub>0-∞</sub> (ng. h/mL)   | 18664.43±1324.18 | 20406.87±1398.42 | 31630.63±1482.66 <sup>@***</sup> |
| AUMC <sub>0-24h</sub> (ng. h <sup>2</sup> /mL)  | 163568±3801.65   | 174534±4238.12   | 254746±4721.08                   |
| MRT <sub>0-24h</sub> (h)  | 9.15±1.02        | 9.01±2.32        | 8.71±1.24                        |
| % RB <sub>(0-24h)</sub>   | 100±0.00         | 107.3±1.23       | 163.96±1.38                      |
| % RB <sub>(0-∞)</sub>   | 100±0.00         | 109.33±1.26      | 169.47±1.42                      |
| Symbols and statistical representations = *** $p < 0.001$ ; @ = compared to pure Eze and Eze-NA (One way ANOVA followed by Tukey's post hoc test). % RB = % Relative bioavailability with respect to pure drug. |                  |                  |                                  |

Pharmacokinetic study was performed to quantify the total plasma Eze concentration (free plasma Eze + plasma EzeG) following single dose oral administration of pure drug suspension and CoCs as 0.25% w/v NaCMC dispersions to male Albino Wister rats.

Eze gets rapidly absorbed after oral administration and is primarily conjugated by the UDP-glucuronosyltransferases (UGT) in the small intestine and liver to EzeG. Like Eze, its glucuronide is also pharmacologically active and is known to be more potent in inhibiting the cholesterol transport than the parent compound. Eze and its glucuronide are the major drug-derived compounds in plasma and account to approximately 10–20% and 80–90% of the total drug in plasma, respectively. The drug quantification by HPLC-UV method was enhanced by incorporating an enzyme hydrolysis step where EzeG was back converted to Eze by the use of the enzyme,  $\beta$ -glucuronidase and the total Eze was estimated. Addition of 25  $\mu$ L  $\beta$ -glucuronidase (minimum 100,000 units/mL) to the plasma samples aided in the conversion of EzeG to Eze and the total Eze in plasma was estimated and reported.

The  $T_{\max}$  was observed in the order, pure drug = Eze-NA > Eze-ND. The  $T_{\max}$  of both, pure drug and Eze-NA was seen at 2 h and that of Eze-ND was recorded at 1 h. Eze-ND reduced the  $T_{\max}$  of pure Eze by half. The parameters,  $C_{\max}$ ,  $AUC_{0-24h}$ ,  $AUMC_{0-24h}$  and  $AUC_{0-\infty}$  were observed in the order, Eze-ND > Eze-NA > pure drug. Eze-ND and Eze-NA improved the mean  $C_{\max}$  of Eze by 2.2 and 1.2 times, respectively. The  $C_{\max}$  of Eze-NA was higher than pure Eze, though, not significantly ( $p > 0.05$ ); the  $C_{\max}$  of Eze-ND was significantly higher ( $p < 0.001$ ) than both, pure Eze and Eze-NA. The  $AUC_{0-24h}$  of Eze-NA was higher compared to pure Eze and the  $AUC_{0-24h}$  of Eze-ND was higher than pure Eze as well as Eze-NA. The same order of performance was observed for the  $AUMC_{0-24h}$  values of pure Eze, Eze-NA and Eze-ND. Both, the mean  $AUC_{0-24h}$  and the mean  $AUMC_{0-24h}$  of Eze were improved by 1.6 and 1.1 times, respectively, by Eze-ND and Eze-NA. The  $AUC_{0-\infty}$  of Eze-NA was higher compared to pure Eze, though, not significantly ( $p > 0.05$ ); the  $AUC_{0-\infty}$  of Eze-ND was far significantly higher ( $p < 0.001$ )

than pure Eze and Eze-NA. Eze-ND and Eze-NA improved the mean  $AUC_{0-\infty}$  of Eze by 2 and 1.1 times, respectively. Insignificant differences were observed in the MRT values of pure drug, Eze-NA and Eze-ND. The plasma concentration time profiles were shown in Figure 5.23.

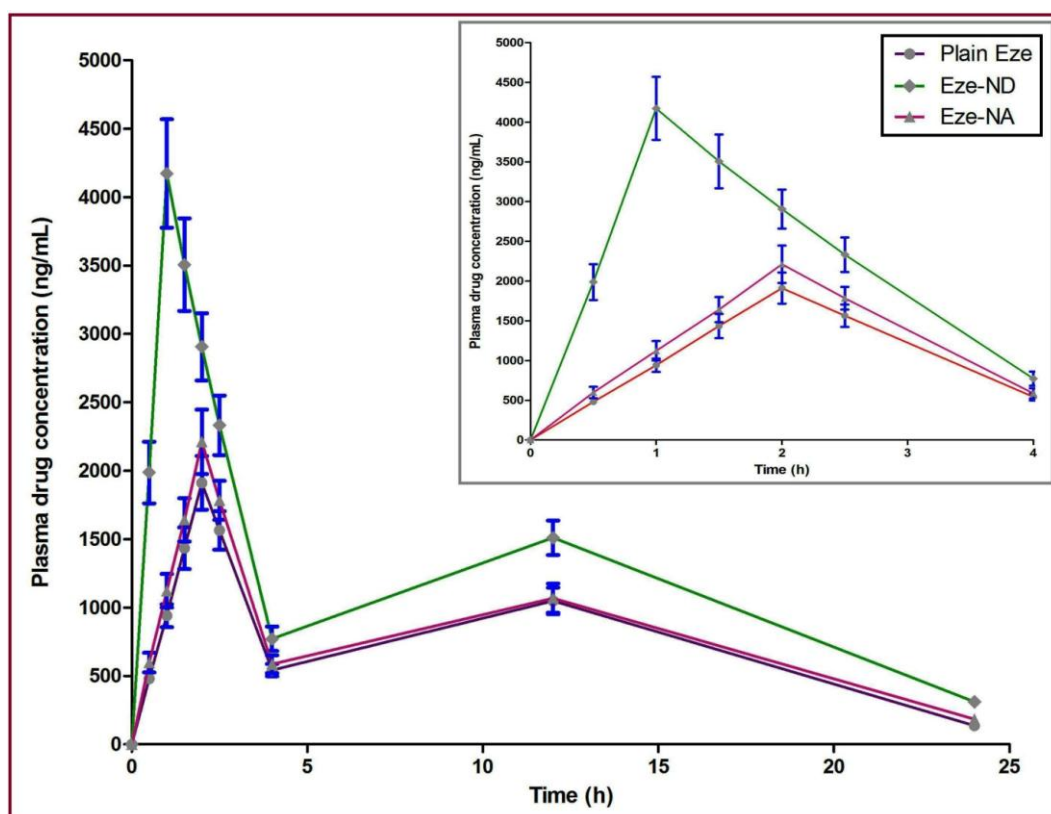


**Figure 5.23. Pharmacokinetic profiles of pure Eze and optimized CoCs (vertical bars represent SD, n = 6). Inset shows the profile up to 4 h.**

The plasma concentration time profile of Eze from the drug suspension and both the CoCs showed that Eze reached its peak followed by a rapid decline and this pattern reoccurred producing multiple peaks in the plasma concentration time graph. These multiple peaks were observed on account of the enterohepatic recirculation underwent by Eze. Following oral absorption, Eze undergoes extensive glucuronidation to a phenolic glucuronide in the intestine and is then excreted into the bile. Due to

enterohepatic recirculation, Eze, after undergoing reabsorption in the ileum, is repeatedly delivered back to its site of action, the intestinal tract lumen. This reabsorption and recirculation processes aided in enhancing the residence time of Eze in the intestinal tract lumen and thus, improved the cholesterol-lowering activity of the drug [Bali et al., 2010 and 2011].

The CoCs presented enhanced bioavailability in comparison to the pure drug which may be attributed to the enhanced solubility which could have led to availability of higher volume of soluble drug in the GIT and thereby, improved absorption.

The  $T_{max}$  of Eze-ND was noted at 1 h while that of Eze-NA and pure drug suspension were observed at 2 h. The reduction in the value of  $T_{max}$  observed for Eze-ND could be due to the fact that the involved coformer for this CoC, ND is known for its high water solubility and hydrophilicity. The involvement of this hydrophilic coformer in the same crystal lattice as Eze, in case of Eze-ND, could have presented Eze in a more soluble form to the GIT. Both the CoCs could have presented the drug for absorption without a need for a lengthy drug dissolution process, dissolution being the major rate-limiting step for gastrointestinal absorption. This fact was quite evident from the dissolution profiles where both the CoCs improved Eze dissolution drastically. However, the relatively low soluble NA could not serve to improve the  $T_{max}$  of Eze as the solubility enhancement offered by the coformer NA could not have presented the Eze-NA CoC in a solubilized form sufficient to reduce the duration of drug dissolution process as effectively as ND coformer or the corresponding CoC, Eze-ND. In case of pure drug suspension, the drug is suspended in the form of fine particles and is yet to undergo dissolution in GIT fluids to get absorbed and hence, the longer  $T_{max}$ . MRT is an intrinsic

property of a drug and there was no change in the intrinsic property of Eze when the drug was formulated into CoCs [Bali et al., 2010 and 2011].

The CoCs of Eze presented enhanced bioavailability due to the increased solubility and immediate drug dispersion of Eze from these formulations in the GIT. Eze-ND, in particular, could have served in improving the intestinal membrane concentrations of solubilized Eze to a higher extent and thus resulted in greater oral absorption of the drug.

#### **5.4.2.9 Antihypercholesterolemic activity**

##### **5.4.2.9.1 Principle behind performing the plasma cholesterol determination test for pure Eze and formulations**

Eze is the first antihypercholesterolemic drug that blocks the Niemann–Pick C1-Like 1 protein in the enterocytes of the intestine, and inhibits cholesterol absorption. It is a selective cholesterol absorption inhibitor, which potently inhibits the absorption of biliary and dietary cholesterol from the small intestine. Mechanistically, Eze reduces the small intestinal enterocyte uptake and absorption of cholesterol and thus keeps the cholesterol in the intestinal lumen for excretion. Eze is rapidly absorbed and primarily metabolized in the small intestine and liver to its glucuronide, both of which undergo enterohepatic recycling. Both, Eze and EzeG are pharmacologically active antihypercholesterolemics [Catapano, 2001].

In the research work described in this chapter, the poor bioavailability of Eze was improved by preparing CoCs with NA and ND. The CoCs improved the solubility, dissolution and bioavailability of pure Eze and the CoCs were further tested to study their effect on the antihypercholesterolemic activity of the drug.

Blood cholesterol is usually determined in serum, and it is generally accepted that the concentration in serum and the concentration in the circulating plasma are identical. Collection of serum is a time taking process compared to plasma separation and therefore, most of the determinations reported in literature were actually made in plasma. So is the reason why the term “plasma cholesterol concentration” is frequently used. In general, anticoagulants exert osmotic effects in which water leaves the cells and enters the plasma, thus diluting the plasma and lowering the concentrations of non diffusible components. The magnitude of this effect depends on the anticoagulant used and its concentration. Heparin in liquid form was established to be the best anticoagulant for use in plasma collection in order to ensure the similar ( $p > 0.001$ ) cholesterol concentration as in serum [Grande et al., 1964].

The cholesterol test system employed in this study is the most common enzymatic method that works based on Trinder reaction which involves the breakdown of cholesterol esters to free cholesterol by cholesterol esterase. Cholesterol oxidase (CHOD), in the presence of oxygen, oxidizes free cholesterol to form cholest-4-ene-3-one and hydrogen peroxide. The hydrogen peroxide reacts with phenol and 4-aminoantipyrine in the presence of peroxidase (POD) to form a quinoneimine dye. The resulting color may be measured by UV-VIS spectrophotometry [<http://www.fda.gov/MedicalDevices/DeviceRegulationandGuidance/GuidanceDocuments/ucm094140.htm>].

Cholesterol, being water insoluble, it is transported in the blood in combination with specific proteins as complexes known as lipoproteins. These lipoproteins are classified as chylomicrons, very low density lipoproteins, low density lipoproteins, intermediate density lipoproteins and high density lipoproteins, and they differ in terms of both

protein and relative lipid composition. The total cholesterol values reflect the total amount of cholesterol in the lipoproteins, and are determined by chemical or enzymatic methods. The specimen used may be whole blood, serum or plasma using either heparin or EDTA as anticoagulant (cholesterol measurements should not be determined from fluoride, citrate, or oxalate treated specimens).

There are problems with using solid or other liquid form anticoagulants for cholesterol test. Some of the anticoagulants commonly used in the preparation of plasma for analysis, when added in the solid form to the blood, induce changes in the distribution of water between cells and plasma. Passage of water from the cells to the plasma causes dilution of the latter, lowering its cholesterol concentration. Serum cholesterol and triglyceride concentrations are about 3-5% higher in serum than in EDTA plasma, although no significant serum - EDTA plasma difference was observed for high density lipoprotein cholesterol. Total cholesterol and triglyceride concentrations are lower in plasma than in serum, apparently because the anticoagulant, disodium EDTA, causes an osmotic redistribution of water between cells and plasma, a redistribution reflected by changes in hematocrit produced by the anticoagulant. It has been reported that plasma from oxalated blood had lower cholesterol concentration than either the serum or the heparinized plasma of the same blood sample. It has been confirmed that the differences in cholesterol concentration between the heparinized and the oxalated plasma were of practical significance. Only heparin used as anticoagulant in liquid form for plasma samples ensured the similar ( $p > 0.001$ ) cholesterol concentration as in serum. Even heparin when used in solid form, prepared either by drying a solution of heparin in distilled water or by drying a commercial solution of heparin in 0.9% NaCl caused some

difference in plasma cholesterol concentrations as compared to liquid form heparin or serum ( $p < 0.01$ ).

Only commercially available solution of heparin was reported not to affect plasma cholesterol concentration. No changes of water distribution between cells and plasma may be expected if commercially available solution of heparin was used. It has been established in the literature that the cholesterol values from liquid form heparinized plasma were essentially similar to those of serum and hence the cholesterol determinations in the present study were conducted using heparinized plasma samples [Grande et al., 1964].

#### **5.4.2.9.2 Hypocholesterolemic potential of pure drug and optimized formulations**

The study was conducted for a total of eight weeks wherein the first four weeks, all the animal groups were fed with 200 mg cholesterol in 2 mL coconut oil as high fat diet for inducing hypercholesterolemia. At the end of fourth week, the plasma cholesterol levels were measured for all the groups and the values were considered as baseline values for the following four week study, the actual antihypercholesterolemic activity study. It was noted that all the animals together showed a mean 80-85% elevation in total plasma cholesterol levels at the end of four week hypercholesterolemic induction study, when compared to day one mean value.

The results of the study were presented in Figure 5.24 and Table 5.11. The antihypercholesterolemic activity of pure Eze or pure NA was statistically insignificant compared to control group ( $p > 0.05$ ). The activity of Eze-NA PM was statistically insignificant, compared to control on days, 7 and 14 ( $p > 0.05$ ), and on all test days ( $p > 0.05$ ) against, pure Eze or pure NA. The cholesterol reducing efficiency of Eze-NA PM



was higher than control ( $p < 0.05$ ) on days 21 and 28. The performances of Eze-NA and Eze-ND were significantly prominent when compared to either control ( $p < 0.001$ ) or pure Eze ( $p < 0.001$ ), or pure NA ( $p < 0.001$ ) or Eze-NA PM ( $p < 0.001$ ) on all the test days. The superior *in-vitro* solubility and dissolution profiles support the remarkable *in-vivo* performance of both the CoCs. However, the difference in the percent reduction in total plasma cholesterol levels achieved by Eze-NA and Eze-ND was statistically insignificant ( $p > 0.05$ ) on all the test days.

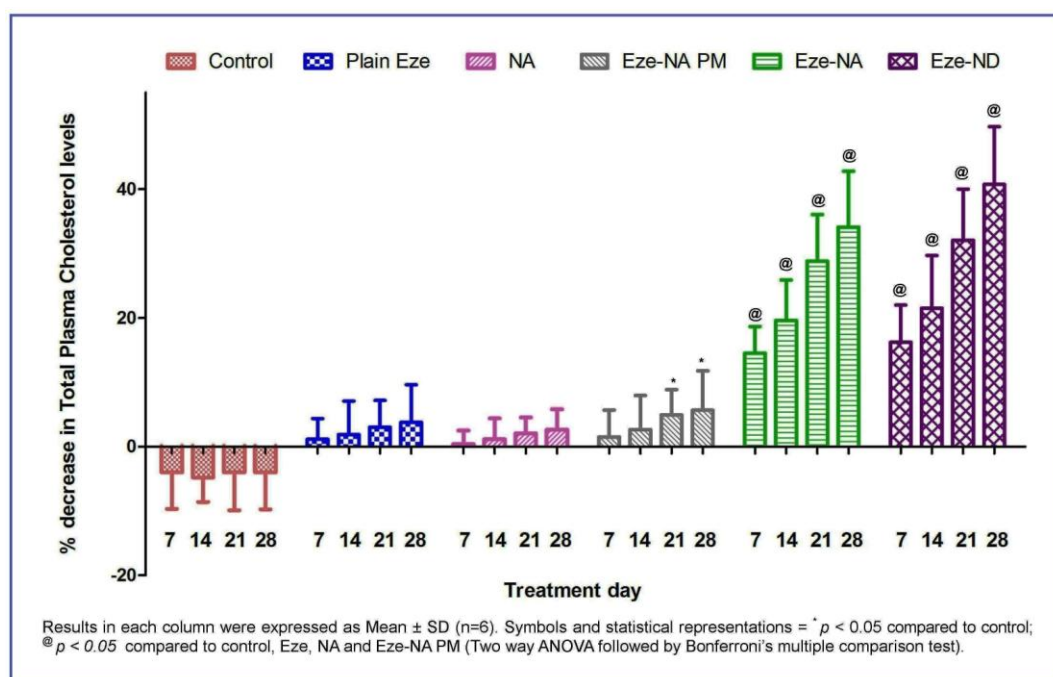


**Figure 5.24. Percent reduction in the total cholesterol levels achieved by pure Eze and CoC formulations (vertical bars represent SD, n = 6).**

As NA is also known for its cholesterol reducing nature, two treatment groups were studied, one treated with NA alone and the other with Eze-NA PM to evaluate the influence of this excipient cofomer on the antihypercholesterolemic activity of Eze-NA

CoC formulations. The study showed that the cholesterol reduction efficiency of Eze-NA CoC was far superior compared to pure Eze or pure NA or Eze-NA PM.

**Table 5.11. Percent reduction in the total cholesterol levels achieved by pure Eze and CoC formulations. Results were expressed as Mean±SD (n = 6).**

| Treatment/Day    | % Decrease in total plasma cholesterol levels |                            |                            |                            |
|------------------|---|----------------------------|----------------------------|----------------------------|
|                  | Day 7   | Day 14                     | Day 21                     | Day 28                     |
| <b>Control</b>   | -4±5.67                                       | -4.8±3.78                  | -4±5.89                    | -4±5.75                    |
| <b>Eze</b>       | 1.13±3.21                                     | 1.89±5.18                  | 3.02±4.16                  | 3.77±5.84                  |
| <b>NA</b>        | 0.377±2.12                                    | 1.132±3.26                 | 2.08±2.48                  | 2.64±3.18                  |
| <b>Eze-NA PM</b> | 1.51±4.16                                     | 2.64±5.28                  | 4.91±3.96 <sup>a*</sup>    | 5.66±6.12 <sup>a*</sup>    |
| <b>Eze-NA</b>    | 14.51±4.16 <sup>b***</sup>                    | 19.61±6.28 <sup>b***</sup> | 28.82±7.24 <sup>b***</sup> | 34.12±8.68 <sup>b***</sup> |
| <b>Eze-ND</b>    | 16.23±5.76 <sup>b***</sup>                    | 21.51±8.18 <sup>b***</sup> | 32.08±7.92 <sup>b***</sup> | 40.75±8.96 <sup>b***</sup> |

Symbols and statistical representations = \*\*\* $p < 0.001$  and \* $p < 0.05$ ; a = compared to Control; b = compared to Control, Eze, NA and Eze-NA PM (Two way ANOVA followed by Bonferroni's post hoc test).

Though Eze-ND presented superior solubility and dissolution compared to Eze-NA, the hypocholesterolemic potentials of Eze-NA and Eze-ND were similar because of the plausible agonistic pharmacological activity of NA with Eze. Both Eze and NA could have produced the antihypercholesterolemic effect in case of Eze-NA which had 1:2 loads of Eze and NA in its crystal lattice. On the other hand, ND is not known for any lipid lowering activity. However, the higher water solubility of ND resulted in superior solubility and dissolution properties of Eze-ND which could have maintained the levels of Eze sufficient to achieve the percent reduction in total plasma cholesterol levels similar to Eze-NA system. Though the pharmacological performances of Eze-NA and

Eze-ND were similar, considering the markedly superior *in-vitro* solubility and dissolution, Eze-ND should be seen as a more promising formulation to reduce the oral bioavailability variations of Eze.

### 5.5 SUMMARY

The present investigation identified two novel CoCs of Eze using NA and ND as coformers and the crystal engineering technique proved promising in improving the aqueous solubility and release properties of Eze. Solid-state materials may be either single component or multi-component with multi-component being further classified into groupings such as host–guest compounds, molecular salts, hydrate/solvates and CoCs. The newly formed crystalline phases of Eze cannot be seen as Eze polymorphs because a polymorph is a single component system with only the API within the crystal lattice. A pharmaceutical CoC is composed of an API and an appropriate coformer. The CoCs generated in this study were stoichiometric systems (confirmed by phase solubility, Job's plotting and stoichiometric assay studies) of an API and coformer. The newly formed crystalline phases of Eze cannot be seen as host–guest compounds because no any cyclodextrin like cavity involved components were employed in this study in order to captivate other components of the system. The newly formed crystalline phases of Eze cannot be seen as molecular salts because the FTIR analysis confirmed the non-existence of any new peaks in the spectra of CoCs. Some of the principle absorption bands of parent components disappeared in the spectra of CoCs but none exhibited new peaks dismissing the possibility of formation of chemical bonds during cocrystallization. Formation of molecular salts involves chemical bonding. The CoC systems described in this work were bonded by pure physical non-ionic and non-

covalent interactions. Besides the CoCs generated in this study contained parent components that were neutral solids under ambient conditions and were connected by supra/ intermolecular interactions. The newly formed crystalline phases of Eze cannot be seen as hydrate/solvates because no weight loss corresponding to solvents was observed in the TGA graphs of either of the CoCs.

Eze-NA and Eze-ND CoCs were successfully designed and prepared by solution crystallization technique on the basis of their solution state phase solubility and Job's plot studies both of which indicated the ratio of their drug:coformer to be 1:2 and 1:1, respectively. FTIR study indicated lack of chemical reaction and suggested intermolecular hydrogen bonding as the possible supramolecular interaction between the CoC components. DSC and PXRD analyses offered confirmation for the generation of new CoC forms with distinguished crystal structure, shape and habit compared to their respective parent components. SEM photographs further confirmed the altered morphology and size of CoCs in comparison to their respective parent components. Both, Eze-NA and Eze-ND CoCs showed marked improvement in flow properties, aqueous solubility and dissolution properties of Eze ( $p < 0.05$ ). Though it was conceived that the preparation of NA CoC of Eze would not only enhance the solubility and dissolution properties of Eze but may also provide an agonistic effect in the treatment of hypercholesterolemia, the results of *in-vitro* characterization suggested ND as a more beneficial coformer. ND, being the higher water soluble coformer, Eze-ND CoCs exhibited superior solubility, dissolution and pharmacokinetic behavior compared to Eze-NA ( $p < 0.05$ ). Though the difference in antihypercholesterolemic ability of both the CoCs was statistically insignificant, considering the statistically superior solubility, dissolution and pharmacokinetics of Eze-ND in comparison to Eze-NA, the former may

be noted as the most effective formulation. Eze-ND may be considered as a potential alternative for the oral delivery of Eze.

## 5.6 GRAPHICAL SUMMARY

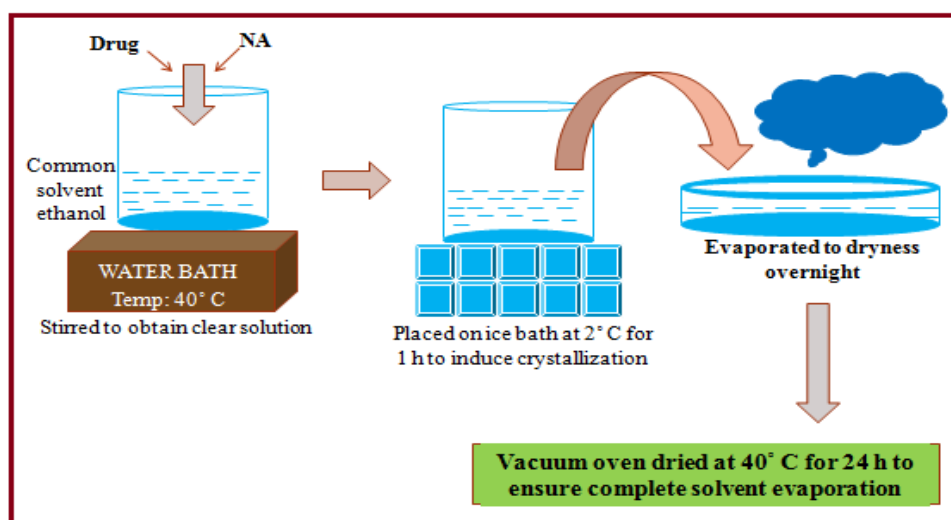


Figure 5.25. Schematic diagram showing formation of Eze-NA.

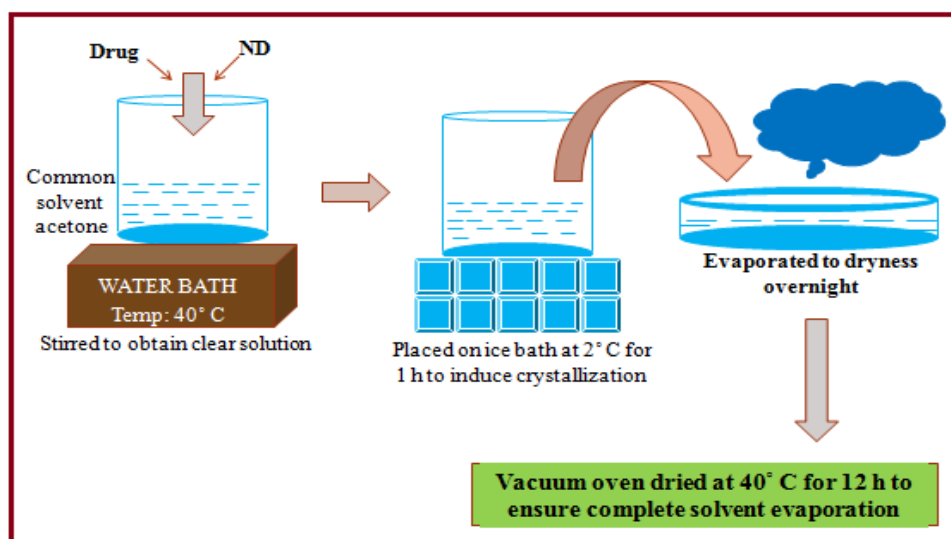


Figure 5.26. Schematic diagram showing formation of Eze-ND.

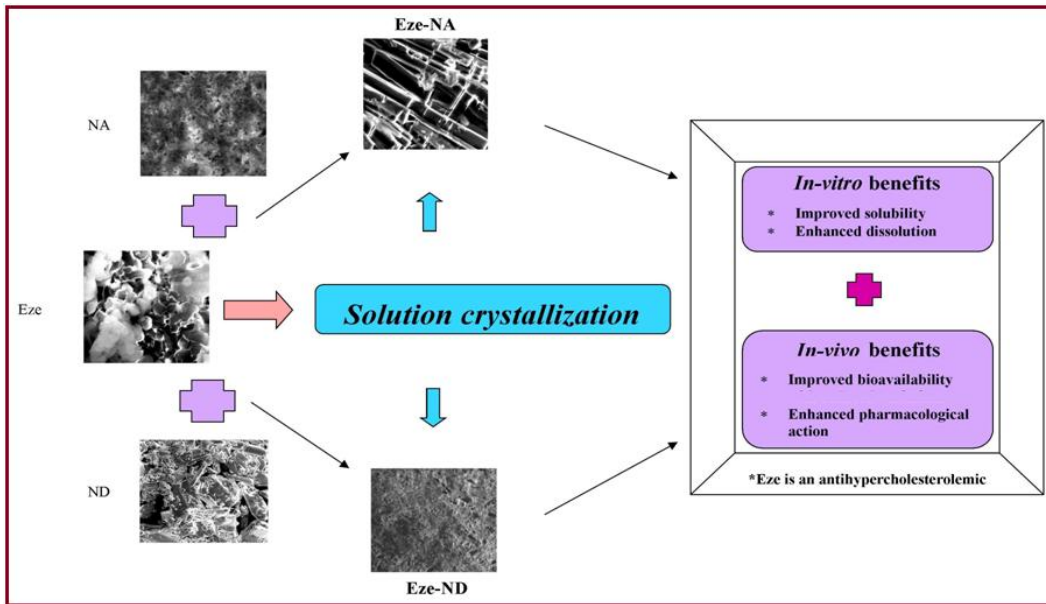


Figure 5.27. Gist of effect of cocrySTALLIZATION formulation approach on Eze performance.

